JACS
JOURNAL OF THE AMERICAN CHEMICAL SOCIETY
Article
pubs.acs.org/JACS

Reactivity of Ruthenium Phosphido Species Generated through the Deprotonation of a Tripodal Phosphine Ligand and Implications for Hydrophosphination

Peter E. Sues, Alan J. Lough, and Robert H. Morris*

Department of Chemistry, University of Toronto, Toronto, Ontario M5S 3H6, Canada

Supporting Information

ABSTRACT: The fragmentation of the 1,1,2-tris(diphenylphosphino)ethane ligand in [RuCp*((Ph$_2$P)$_2$CHCH$_2$PPh$_2$)][PF$_6$] (**1**) was explored through treatment with base under aprotic conditions. The neutral phosphido complex RuCp*(PPh$_2$CH=CHPPh$_2$)(PPh$_2$) (**2**) with a (*Z*)-1,2-bis(diphenylphosphino)ethene (dppen) ligand was generated through a base-facilitated dehydrophosphination reaction. Installation of a bis(*p*-tolyl)phosphido ligand was attempted by combining bis(*p*-tolyl)phosphine with RuCp*(dppen)Cl in the presence of KO*t*Bu, but surprisingly, the unsymmetrical diphenylphosphido compound RuCp*(Ph$_2$PCHCHP(*p*-tol)$_2$)(PPh$_2$) (**5**) was generated instead. The ligand rearrangement reaction was driven by the greater electron density on the bis(*p*-tolyl)phosphido moiety. Density functional theory calculations showed that fragmentation to the 1,2-disubstituted ligand was thermodynamically favored over the 1,1-disubstituted ligand and that intramolecular phosphido exchange was kinetically accessible at room temperature. The greater basicity of the bis(*p*-tolyl)phosphido ligand was experimentally verified by the measured pK_a^{THF} of 28 for the acid/base pair [RuCp*(Ph$_2$P(*o*-C$_6$H$_4$)PPh$_2$)(P(*p*-tolyl)$_2$H)]$^+$/RuCp*(Ph$_2$P(*o*-C$_6$H$_4$)PPh$_2$)(P(*p*-tolyl)$_2$) versus 25 for the acid/base pair [RuCp*(Ph$_2$P(*o*-C$_6$H$_4$)PPh$_2$)(PPh$_2$H)]$^+$/RuCp*(Ph$_2$P(*o*-C$_6$H$_4$)PPh$_2$)(PPh$_2$) (**7**). For comparison, the approximate pK_a^{THF} values for free P(*p*-tolyl)$_2$H/[K(crypt)]P(*p*-tolyl)$_2$ and free PPh$_2$H/[K(crypt)]PPh$_2$ are 43 and 38, respectively. This is the first quantitative measurement of the large effect that coordination to a metal center, in this case ruthenium(II), has on the acidity of secondary phosphines. This is useful information for designing and understanding hydrophosphination catalysts. Complexes **2** and **7** are catalysts for the addition of PPh$_2$H to acrylonitrile, but they deactivate fairly rapidly. The pK_a^{THF} measurements are consistent with a catalytic cycle involving a Michael addition step. Complex **2** in solution underwent a slow, unprecedented rearrangement of P−C, C−C, and C−H bonds to give crystalline Ru(C$_5$(CH$_3$)$_4$(CH$_2$C$_6$H$_5$))(Ph$_2$PCH$_2$CH$_2$PPh(*o*-C$_6$H$_4$)PPh) (**9**) in high yields, demonstrating the unpredictable reactivity of phosphido ligands.

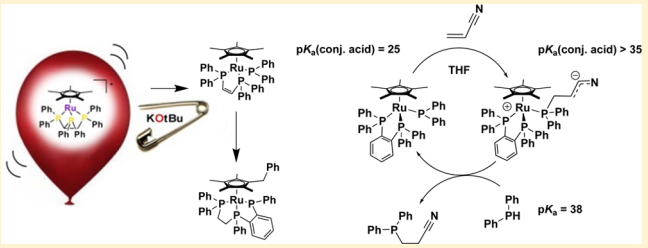

INTRODUCTION

The coordination chemistry of negatively charged deprotonated secondary phosphines, or phosphido ligands, is incredibly diverse, and the reactivity of these ligands is contingent on their specific coordination mode.[1] Bridging phosphidos, which form relatively stable metal clusters or bimetallic species, tend to be less reactive because both lone pairs on phosphorus are occupied in metal−phosphorus bonds,[1−12] whereas trigonal-pyramidal phosphidos or terminal phosphidos, where the phosphorus atom is bound to only one metal center, are much more nucleophilic because of their unquenched lone pair.[1,13−21] As such, terminal phosphidos are known to react with various electrophiles, including HX, MeI, and Et$_3$SiH, among several other reagents.[15,16,22−26] The third possible coordination mode for phosphidos occurs when a metal ion would otherwise be coordinatively unsaturated without additional bonding from the phosphorus-based ligand.[1,17,27−35] In this case, the lone pair on phosphorus forms a π bond with the metal center and the phosphido adopts a trigonal-planar geometry. Despite the metal−phosphorus double bond, planar phosphidos have reactivity similar to that of terminal phosphidos in that they are very basic and nucleophilic; they have even been reported to deprotonate phenyl groups.[17,28,36]

Phosphido ligands are especially important in the late-transition-metal-catalyzed hydrophosphination of unsaturated substrates, as conventional organometallic catalytic mechanisms involve the insertion of an alkene or alkyne into the M−P bond of a phosphido intermediate.[22−26,37−59] A typical organometallic mechanism for alkene hydrophosphination involves oxidative addition of a primary or secondary phosphine to an electron-rich metal center followed by coordination of the olefin substrate and subsequent insertion to form a P−C bond (Scheme 1).[22−26,37,38,41,42,44,47,48,50−63] Reductive elimination of the hydride and alkyl moieties completes the catalytic cycle, generating the hydrophosphinated product and recovering the electron-rich metal center (Scheme 1).[22−26,37,38,41,42,44,47−63]

Received: January 27, 2014
Published: February 25, 2014

   dx.doi.org/10.1021/ja5006724 | *J. Am. Chem. Soc.* 2014, 136, 4746−4760

Scheme 1. (Right) Organometallic and (Left) Michael Addition Mechanisms for the Hydrophosphination of Alkenes[22−26,37,38,41,42,44,47,48,50−63]

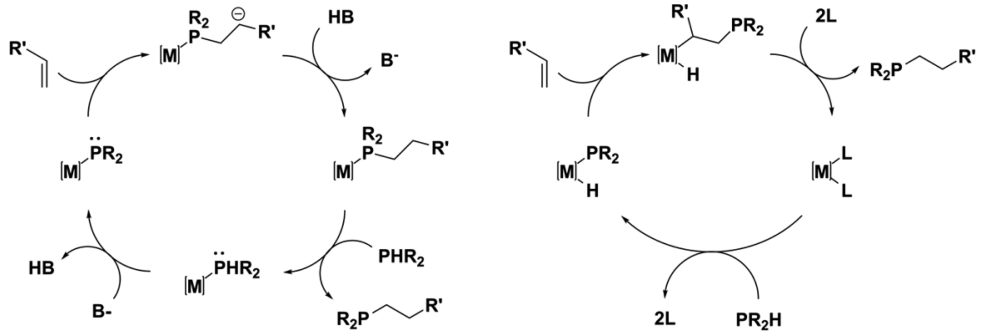

Another possible mechanism for hydrophosphination that also includes metal phosphido intermediates is a Michael addition route, where attack of the phosphido ligand on an alkene is followed by protonation of the resulting carbanion (Scheme 1).[22−26,37,38,41,42,44,47−54,56−63] Subsequent coordination and deprotonation of a phosphine then closes the catalytic cycle. Exploring the behavior and reactivity of phosphido ligands is therefore crucial for better understanding either an organometallic or Michael addition mechanism of hydrophosphination as well as for developing more efficient and selective catalytic systems.

In this paper, we explore the fragmentation of the 1,1,2-tris(diphenylphosphino)ethane (tppe) ligand in [RuCp*(tppe)][PF_6] (**1**) upon treatment of the cationic ruthenium complex with KO*t*Bu under aprotic conditions. The base facilitates dehydrophosphination of the tppe ligand, producing a deprotonated ruthenium phosphido species. In addition, we examine the unexpected exchange of a phosphido ligand with a phosphine moiety of an "inert" bidentate phosphine ligand and compare the measured pK_a values of free and coordinated secondary phosphines in order to understand the high nucleophilicity of phosphido groups here and in catalytic hydrophosphination reactions. Lastly we discuss a remarkable rearrangement of the deprotonated ruthenium complex, which illustrates the diverse and sometimes unpredictable reactivity of phosphido ligands.

RESULTS AND DISCUSSION

Deprotonation of Parent Complex 1 To Yield Complex 2. The previously reported ruthenium complex **1** was found to be air- and moisture-stable as well as completely unreactive toward small molecules, even at elevated temperatures.[64] However, reaction with a strong base such as KO*t*Bu or KH under aprotic conditions (in THF, toluene, or benzene) caused a dramatic color change from light yellow to deep red. Upon further inspection, the reaction with base resulted in quantitative conversion of the parent compound into a new deprotonated species, **2**, (Scheme 2) which could be isolated as a brick-red powder in excellent yield (94%).

The NMR spectra of **2** signaled the formation of *cis*-1,2-bis(diphenylphosphino)ethene (dppen, also known as dppv) and diphenylphosphido ligands, suggesting that deprotonation occurred at the disubstituted carbon instead of the trisubstituted carbon and caused an elimination reaction to occur within the ruthenium complex. The $^{31}P\{^1H\}$ NMR spectrum of the parent complex **1** displayed a triplet at 60.8 ppm and a doublet at 39.8 ppm for the single inequivalent phosphorus donor and the two equivalent phosphorus donors,

Scheme 2. Synthesis of the Ruthenium Half-Sandwich Phosphido Species 2

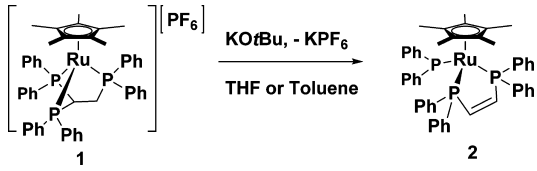

respectively. Upon deprotonation, a doublet representing the dppen phosphorus nuclei appeared downfield at 79.2 ppm, while the triplet representing the phosphido donor was upfield at 23.2 ppm. If deprotonation of the trisubstituted carbon had occurred without carbon−phosphorus bond cleavage, then the signal for the equivalent phosphines would remain upfield because of the adjacent localized negative charge, as was seen by Ruiz and co-workers.[65,66] Examination of the two-dimensional (2D) gradient heteronuclear single-quantum coherence (gHSQC) spectrum revealed the presence of alkene carbons at 147 ppm in the ^{13}C NMR spectrum correlated to vinylic protons at around 7.3 ppm in the ^1H NMR spectrum (no methylene protons were detected). This identified the presence of the dppen unsaturated ligand backbone, while the chemical shift at 23.2 ppm in the $^{31}P\{^1H\}$ NMR spectrum was diagnostic of a phosphido ligand (this value is consistent with the chemical shifts seen by the Gladysz group for similar ruthenium half-sandwich phosphido complexes[18]).

Base-induced bond cleavage to produce a phosphido ligand is a process similar to other phosphorus−carbon bond cleavage reactions known in the literature.[67−71] Moreover, the KO*t*Bu-promoted dehydrophosphination of the tppe ligand is the reverse of several related hydrophosphination reactions.[41,44]

X-ray diffraction (XRD) studies revealed that complex **2** adopts a distorted-piano-stool geometry in which the Cp* ligand occupies one-half of the coordination sphere while the dppen ligand and a trigonal-pyramidal diphenylphosphido ligand occupy the other three coordination sites (Figure 1). In the parent compound **1** there is a considerable amount of ring strain in the tripodal phosphine ligand, as reflected by the P−Ru−P angles, which are all compressed below the optimal octahedral angle of 90° [P(1)−Ru(1)−P(2), P(1)−Ru(1)−P(3), and P(2)−Ru(1)−P(3) bond angles of 79.0(2), 80.8(2), and 69.4(2)°, respectively].[64] The base-induced elimination of the diphenylphosphido and formation of dppen to give **2**, however, relieves the geometric constraints imposed by the tripodal ligand architecture. This allows the phosphorus donors to move apart and expand the P−Ru−P bond angles: the bidentate phosphine ligand has a P(1)−Ru(1)−P(2) bite angle

dx.doi.org/10.1021/ja5006724 | J. Am. Chem. Soc. 2014, 136, 4746−4760

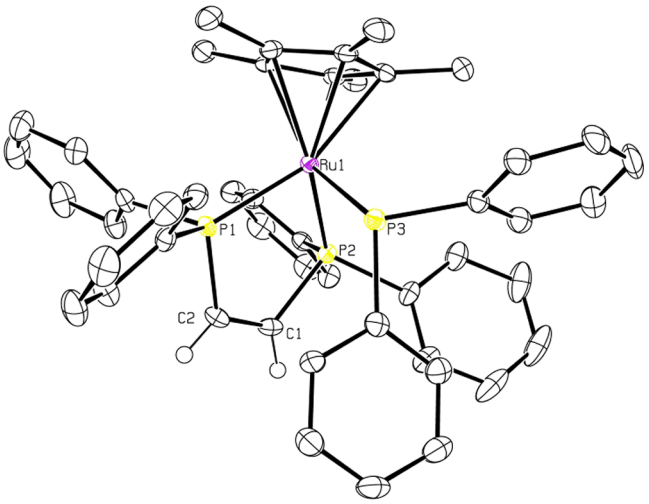

Figure 1. ORTEP3 representation and atom numbering for **2** (thermal ellipsoids at 50% probability; most of the hydrogens omitted for clarity).

of 82.48(9)°, while the P(1)−Ru(1)−P(3) and P(2)−Ru(1)−P(3) bond angles are 91.12(6) and 96.01(6)°, respectively. Furthermore, in the parent complex **1**, all of the Ru−P distances are greater than 2.3 Å, whereas in **2** the Ru(1)−P(1) and Ru(1)−P(2) bond lengths, representing the dppen donors, contract to 2.269(2) and 2.254(2) Å, respectively.[64] Conversely, the Ru(1)−P(3) bond distance lengthens to 2.461(2) Å, which is characteristic of terminal phosphidos (see Table 1 for other notable bond lengths and angles).[14,15,17] The long ruthenium−phosphorus distance is attributed to the "transition-metal gauche effect", in which the lone pair on phosphorus is repelled by a filled d orbital on the metal center, and the conformation that the phosphido ligand adopts minimizes this electronic repulsion as well as steric interactions.[13,14]

Protonation and Regeneration of Complex 2 Using Acid and Base. In order to probe the basicity and nucleophilicity of the phosphido ligand, the deprotonated species was exposed to acid under moisture-free conditions. When a solution of **2** in toluene was treated with an excess of HCl in ether, the cationic diphenylphosphine complex **3** could be isolated as a yellow powder in good yields (77%). Furthermore, complex **2** could be recovered quantitatively from **3** through deprotonation with excess base, indicating that the protonation and deprotonation of the phosphido ligand are completely reversible (Scheme 3).

The ^{31}P and ^{1}H NMR spectra of **3** in THF-d_8 unequivocally demonstrated that protonation occurred at the phosphido

Scheme 3. Acid/Base Reactivity of Complex 2

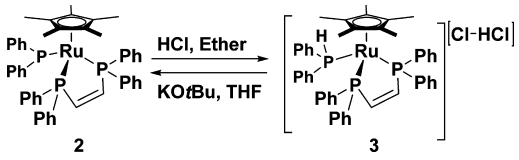

center. In the $^{31}P\{^{1}H\}$ NMR spectrum, the triplet representing the phosphido group shifted downfield from 23.2 ppm in **2** to 37.9 ppm in **3** and displayed a strong P−H coupling (with a coupling constant of J_{P-H} = 357 Hz). In the ^{1}H NMR spectrum, a P−H resonance could also be detected at 6 ppm as a doublet of triplets due to a strong P−H coupling (J_{P-H} = 357 Hz) as well as weaker coupling to the other phosphorus nuclei (J_{P-H} = 6 Hz). In addition, no methylene protons could be detected, and much like **2**, analysis of the 2D gHSQC spectrum revealed the presence of a dppen ligand (olefinic carbons at 146 ppm in the ^{13}C NMR spectrum coupled to vinylic protons at around 7.5 ppm in the ^{1}H NMR spectrum).

Along with NMR experiments, complex **3** was also characterized utilizing XRD. The ruthenium center exhibits a distorted-piano-stool geometry very similar to that of **2**, with Cp* opposite *cis* dppen and diphenylphosphine ligands (Figure 2). Upon protonation of the phosphido ligand, the P−Ru−P

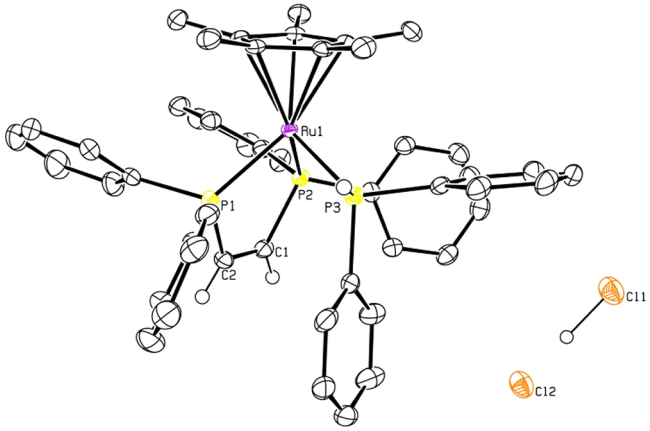

Figure 2. ORTEP3 representation and atom numbering for **3** (thermal ellipsoids at 50% probability; solvent and most of the hydrogens omitted for clarity).

bond angles remain unchanged for the most part (Table 1) while the Ru−P bonds for the dppen ligand lengthen by about 0.04 Å and the Ru(1)−P(3) bond contracts by 0.14 Å [from

Table 1. Selected Bond Lengths (Å) and Angles (deg) for 1, 2, 3, 5, 7, and 9

	1[a]	2	3	5	7	9
			Bond Lengths (Å)			
Ru(1)−P(1)	2.309(5)	2.265(2)	2.301(2)	2.276(3)	2.254(2)	2.269(2)
Ru(1)−P(2)	2.333(6)	2.253(2)	2.302(2)	2.258(3)	2.269(2)	2.254(2)
Ru(1)−P(3)	2.307(6)	2.461(4)	2.324(2)	2.468(3)	2.441(2)	2.366(2)
C(1)−C(2)	1.56(4)	1.316(9)	1.326(9)	1.31(2)	1.40(2)	1.519(9)
			Bond Angles (deg)			
P(1)−Ru(1)−P(2)	79.0(2)	82.48(9)	82.48(6)	82.50(9)	80.94(6)	83.83(6)
P(1)−Ru(1)−P(3)	80.8(2)	91.12(6)	89.19(6)	91.46(9)	97.30(6)	99.53(6)
P(2)−Ru(1)−P(3)	69.4(2)	96.01(6)	97.03(6)	95.87(9)	87.22(6)	83.77(6)

[a]Data from ref 64.

dx.doi.org/10.1021/ja5006724 | J. Am. Chem. Soc. 2014, 136, 4746−4760

2.461(4) Å for the phosphido ligand in **2** to 2.324(2) Å for the phosphine ligand in **3**]. Another feature of note is the presence of the hydrogen dichloride anion, where the additional equivalent of HCl is not removed when the crystals are exposed to reduced pressure. The proton sits between the two chlorine atoms with Cl(1)−HCl(2) and Cl(2)−HCl(1) bond lengths of 1.55(9) and 1.58(9) Å, respectively, which are comparable to the distances for other hydrogen dichloride anions reported in the literature.[72−74]

Alternative Synthesis of 2 and Synthesis of a Bis(*p*-tolyl)phosphino Analogue, Complex 5. Scheme 4 shows a second route to **2** involving a synthesis of phosphido complexes that is more general and versatile than that in Scheme 2. Starting with the commercially available *cis*-dppen ligand and a suitable ruthenium(II) precursor, RuCp*(cod)Cl, the neutral chloride complex **4** was generated in good yield (84%; Scheme 4). The NMR spectra of **4** in CD_2Cl_2 unambiguously showed that coordination of the dppen ligand had occurred (a singlet at 81 ppm in the $^{31}P\{^1H\}$ NMR spectrum, a doublet at 7.5 ppm in the ^1H NMR spectrum representing vinylic protons, and a doublet of doublets at 148 ppm in the ^{13}C NMR spectrum for the olefinic carbons). Removal of the chloride in **4** with AgOTf in THF followed by coordination of diphenylphosphine and then deprotonation with KO*t*Bu afforded **2** in moderate yield (53%; Scheme 4). It should be noted that hydrophosphination of the dppen ligand did not occur upon addition of diphenylphosphine to **4**; instead, **3** was detected by ^{31}P NMR spectroscopy.

Scheme 4. Synthesis of Complexes 2 and 5 via Intermediate Complex 4

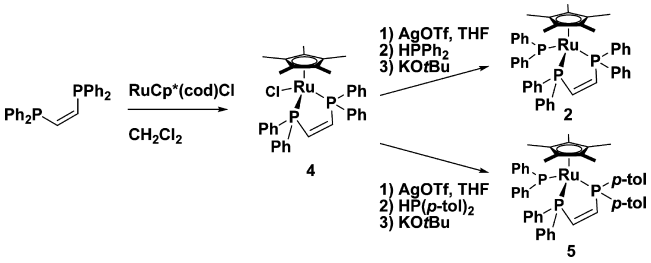

The synthesis of a bis(*p*-tolyl)phosphido analogue of **2** was also targeted by this route. The chloride of **4** was abstracted with AgOTf, and then bis(*p*-tolyl)phosphine was added to the reaction mixture. Upon reaction with KO*t*Bu in THF, the yellow solution turned dark red, and complex **5** was isolated as a red powder in moderate yield (72%; Scheme 4).

XRD studies (Figure 3) revealed that **5** contains a 1-bis(*p*-tolyl)phosphino-2-diphenylphosphinoethene ligand as well as a diphenylphosphido group as a result of an unexpected ligand rearrangement: the bis(*p*-tolyl)phosphino moiety was incorporated into the bidentate ligand at the expense of a diphenylphosphido functionality. This reaction is reminiscent of a transformation seen by the Stradiotto group in which a phosphido exchanged with the amine functionality of a bidentate ligand with an indenyl backbone.[75] The bond lengths and angles of complex **5** were nearly identical to those seen for **2** (Table 1).

The spectroscopic data for **5** were completely consistent with the results from the X-ray diffraction study. Two distinct methyl peaks were observed at 2.4 and 2.3 ppm in the ^1H NMR spectrum for the inequivalent bis(*p*-tolyl)phosphino methyl

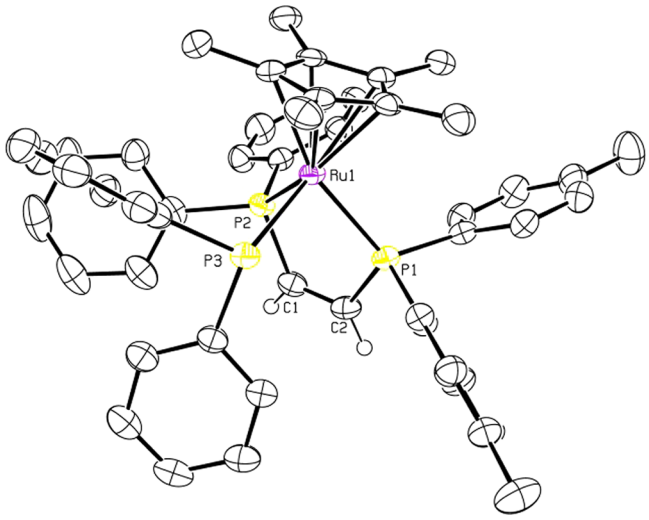

Figure 3. ORTEP3 representation and atom numbering for **5** (thermal ellipsoids at 50% probability; solvent and most of the hydrogens omitted for clarity).

groups. Moreover, resonances for three inequivalent phosphorus nuclei were evident in the $^{31}P\{^1H\}$ NMR spectrum: two doublets of doublets at 79.3 and 78.0 ppm as well as a triplet at 23.0 ppm.

NMR studies of the formation of **5** were also conducted in order to determine whether hydrophosphination of the dppen ligand occurred upon the addition of bis(*p*-tolyl)phosphine to **4** after treatment with AgOTf (i.e., via intermediate **A** in Scheme 5). A ^{31}P NMR spectrum of the reaction mixture showed a strong P−H coupling for the inequivalent phosphorus donor in the crude reaction mixture, indicating that intermediate **A** containing dppen and $P(p\text{-tol})_2H$ ligands (Scheme 5) was present in solution and that swapping of the phosphorus functionalities took place only after the addition of base. We believe that the driving force for this exchange can be attributed to electronic factors relating to the gauche effect. A bis(*p*-tolyl)phosphido is more electron-rich and thus would experience greater repulsion from a filled d orbital on the ruthenium center. By exchange with a less electron-rich diphenylphosphido, the electronic repulsion could be minimized, affording a more stable species. This difference in electron density is reflected by the pK_a of bis(*p*-tolyl)phosphine in THF, which was determined by NMR experiments to be approximately 43 on the basis of the *K* value for the reaction shown in eq 1:

$$\mathrm{HP}(p\text{-tolyl})_2 + [\mathrm{K(crypt)}]\mathrm{NPh}_2 \overset{K}{\rightleftarrows} [\mathrm{K(crypt)}][\mathrm{P}(p\text{-tolyl})_2] + \mathrm{HNPh}_2 \quad (1)$$

where "crypt" denotes 2.2.2-cryptand. This is 5 orders of magnitude more basic than diphenylphosphine in THF ($pK_a \approx 38$, as reported previously).[76] Furthermore, the reaction may also be driven by statistical factors in that the unsymmetrical complex has a higher entropy.

This unanticipated reactivity could have implications for hydrophosphination reactions, where a common goal is to more efficiently produce chiral, multidentate phosphorus ligands from alkene substrates with phosphorus substituents. In most studies, diphenylphosphine is used as a standard substrate, but there are many cases in which more electron-rich phosphines would be preferable, and ligands with different

dx.doi.org/10.1021/ja5006724 | J. Am. Chem. Soc. 2014, 136, 4746−4760

Scheme 5. The Two Possible Intermediates on the Way to Complex 5

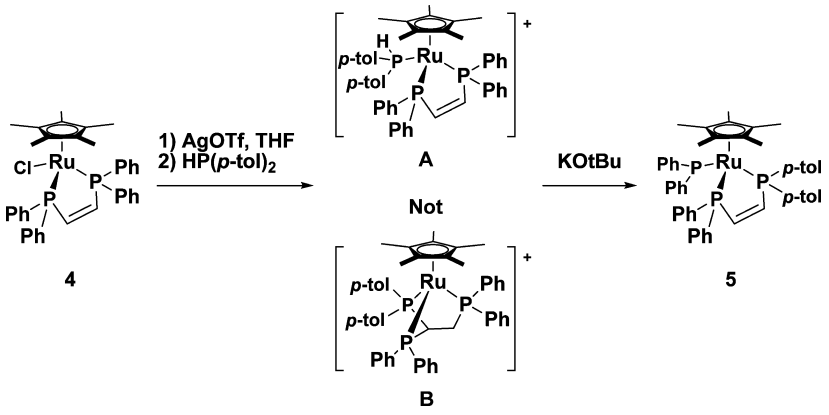

phosphorus donors would also be desirable.[25,26,41,44,61] In these cases, unexpected products could be produced if the substituted olefin and secondary phosphine starting materials are not chosen carefully. It may be important to manage how electron-rich the phosphido ligand is in relation to the other phosphorus donors on the substrate in order to prevent unwanted swapping of phosphorus moieties: the more electron-deficient phosphido ligand should be targeted with the more electron-rich phosphorus functionalities on the olefin.

Synthesis of 1,2-Bis(diphenylphosphino)benzene Analogues, Complexes 6−8. The pK_a values for diphenylphosphine and bis(*p*-tolyl)phosphine in ruthenium(II) complexes were also of interest in order to better understand the facile P−C bond rearrangements seen in the formation of **5** (and **2** as described below) as well as for hydrophosphination reactions in general. Only qualitative studies of this type have been reported to date.[18] To this end, analogues of **2** employing the 1,2-bis(diphenylphosphino)benzene (dppbz) ligand with an aromatic backbone were targeted to prevent the exchange of phosphido ligands with the bidentate donor. By means of an approach similar to that in Scheme 4, dppbz and RuCp*(cod)Cl were combined to generate the neutral chloride species **6** in good yield (77%; Scheme 6). The $^{31}P\{^1H\}$ NMR spectrum was

Scheme 6. Synthesis of *o*-Phenylene Analogues 7 and 8 via Intermediate Complex 6

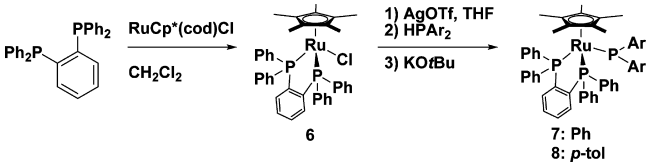

quite diagnostic, with a singlet at 72.1 ppm. With **6** readily available, abstraction of the chloride with AgOTf and coordination of diphenylphosphine followed by deprotonation with KO*t*Bu allowed the facile synthesis of **7** in 87% yield, whereas the use of bis(*p*-tolyl)phosphine gave complex **8** in 76% yield (Scheme 6).

The NMR spectra of complexes **7** and **8** in THF-d_8 were very similar to those of **2**, except that the olefinic carbons and vinylic protons were absent; instead, they were replaced by additional proton signals associated with the aromatic ring. The $^{31}P\{^1H\}$ NMR spectra were especially diagnostic, with doublets at 76.2 and 76.0 ppm, respectively, representing the dppbz phosphorus atoms and broad singlets for the diarylphosphido ligand at 13.1 and 10.7 ppm, respectively. In the case of **8**, the $^{31}P\{^1H\}$ NMR spectrum indicated that the dppbz ligand remained intact while the bis(*p*-tolyl)phosphido endured as a monodentate ligand.

Much like **2**, the XRD structure of the *o*-phenylene analogue **7** (Figure 4) shows a distorted-piano-stool geometry with the

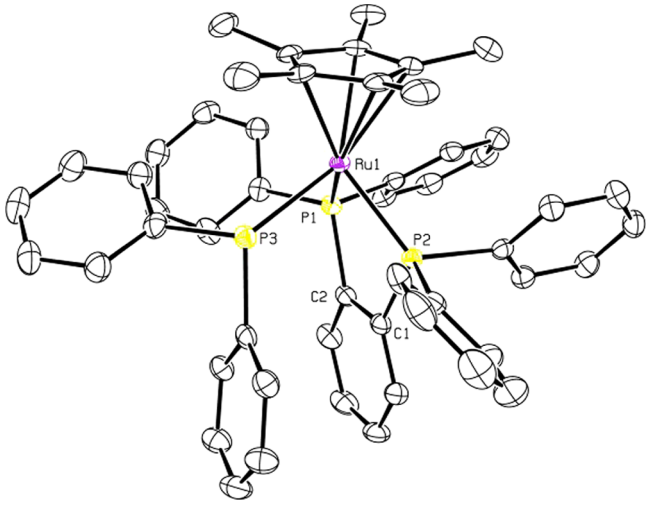

Figure 4. ORTEP3 representation and atom numbering for **7** (thermal ellipsoids at 50% probability; most of the hydrogens omitted for clarity).

dppbz and diphenylphosphido ligands opposite the Cp* ligand (Figure 4). In addition, the P−Ru−P bond angles deviate from the optimal octahedral angle of 90° [80.94(6), 97.30(6), and 87.22(6)° for P(1)−Ru(1)−P(2), P(1)−Ru(1)−P(3), and P(2)−Ru(1)−P(3), respectively]. Compared with **2**, however, the Ru−P distances for the bidentate ligand are slightly longer for **7** [Ru(1)−P(1) and Ru(1)−P(2) bond lengths of 2.254(2) and 2.269(2) Å, respectively] while the Ru(1)−P(3) bond length for the phosphido is slightly shorter [2.441(2) Å] (Table 1). The elongation of the Ru(1)−P(3) bond in comparison with the other Ru−P bonds is attributed again to the gauche effect.

pK_a Studies. The pK_a values for the two dppbz metal complexes **7** and **8** were experimentally determined by $^{31}P\{^1H\}$ NMR spectroscopy through the use of a phosphazenium acid of known pK_a for comparison with the pK_a values for the corresponding free secondary phosphines (Table 2). It was found that the bis(*p*-tolyl)phosphido complex **8** is 3 orders of magnitude more basic than the diphenylphosphido complex **7**.

dx.doi.org/10.1021/ja5006724 | J. Am. Chem. Soc. 2014, 136, 4746−4760

Table 2. Approximate pK_a Values in THF

acid/base	rel. pK_a[a]	abs. pK_a[b]	ref
P(*p*-tol)$_2$H/[K(crypt)][P(*p*-tol)$_2$][c]	2 ± 0.5	43 ± 4	this work
NPh$_2$H/[K(crypt)][NPh$_2$]	0	41 ± 4	ref 76
PPh$_2$H/[K(crypt)][PPh$_2$][c]	−3 ± 0.5	38 ± 4	ref 76
[Ru(Cp*)(dppbz)(P(*p*-tol)$_2$H)]BF$_4$/Ru(Cp*)(dppbz)(P(*p*-tol)$_2$) (**8**)[d]	2 ± 0.5	28 ± 3	this work
[P(NMe$_2$)$_3$NP(NMe$_2$)$_2$NH^{t}Bu]BF$_4$/P(NMe$_2$)$_3$NP(NMe$_2$)$_2$N^{t}Bu	0	26 ± 3	ref 76
[Ru(Cp*)(dppbz)(PPh$_2$H)]BF$_4$/Ru(Cp*)(dppbz)(PPh$_2$) (**7**)[d]	−1 ± 0.5	25 ± 3	this work

[a]The errors in the relative pK_a values are significantly smaller than the errors in the absolute pK_a values because the equilibrium constants were determined under the same conditions with the same acid, and therefore, the errors arise only from the NMR instrument and weighing of the reagents. [b]The errors in the absolute pK_a values are significantly larger than the errors in the relative pK_a values because the errors are accumulated from the entire pK_a^{THF} ladder. See ref 76 for the calculation of the errors in the measured values. [c]The relative pK_a values are referenced to PPh$_2$H/[K(crypt)][PPh$_2$]. [d]The relative pK_a values are referenced to [P(NMe$_2$)$_3$NP(NMe$_2$)$_2$NH^{t}Bu]BF$_4$/P(NMe$_2$)$_3$NP(NMe$_2$)$_2$N^{t}Bu.

This result supports the hypothesis that the formation of **5** is driven by the difference between the electron densities of the two phosphido ligands and that incorporation of the more electron-rich phosphorus donor into the bidentate ligand is favored because it minimizes electronic repulsion due to the gauche effect.

A comparison of the pK_a values in Table 2 reveals that the acidity of the secondary phosphines increases by 13−15 orders of magnitude when they are coordinated to ruthenium in the cationic half-sandwich compounds. These are significant changes considering that the resulting metal complexes are extremely electron-rich with Cp* and three strong σ donors as ligands. For less electron-rich systems, the size of this shift should be even larger. There are some other literature reports of pK_a values of metal−element−hydrogen groups where the hydrogen is two bonds from the metal center.[77,78] The most common are for aqua complexes in water, where the pK_a can drop by up to 15 units when water coordinates to cations with high charge-to-size ratios.[79−81] Similarly, amines, which are very weak acids in water, can have pK_a values near 0 when bound to trivalent cations,[82] whereas ammonia can have a very wide range of pK_a values when bound to metals in non-aqueous solutions, depending on the structure of the complex.[83] Moreover, coordination of an aminoolefin to cationic rhodium(I) resulted in a change of 10 units in pK_a^{DMSO},[84] while the pK_a^{DMSO} of a secondary amine in a cationic iridium(I) complex changed from 22 to 15 upon substitution of only one ligand (PMe_3 to CO).[85] Astruc and co-workers reported that the pK_a^{DMSO} values for the 18-electron complexes [Fe(η^5-C_5R_5)(η^6-C_6Me_6)]$^+$ (R = H, Me) and [Fe(η^5-C_5R_5)(η^6-$C_6H_5CHPh_2$)]$^+$ were found to be 12−14 units lower than the pK_a of the benzylic C−H of the free ligand,[86] while even the pK_a^{MeCN} of 1,3-diketones was found to decrease by 12 units upon coordination to copper(II).[87] Additionally, hydrogen sulfide coordinated in a neutral ruthenium(II) complex was found to be significantly more acidic than free H_2S, whereas thiols, on the other hand, were found to be less affected by metal coordination.[88,89]

Catalytic Hydrophosphination. The ruthenium phosphido complexes **2** and **7** were tested for hydrophosphination and were found to catalyze the addition of diphenylphosphine to acrylonitrile at room temperature (Scheme 7). The former catalyst was twice as active as the latter, but the reactions did not proceed to completion because the active species deactivated rapidly after only 1 h. In comparison with other acrylonitrile hydrophosphination catalysts reported in the literature, complexes **2** and **7** operated more rapidly [turnover frequencies (TOFs) of 30 and 60 h^{-1}, respectively, at room temperature with a catalyst loading of 1% vs a TOF of 10 h^{-1} at 50 °C with a catalyst loading of 10% for a platinum-based system[59]] but deactivated more rapidly as well. In addition, a byproduct similar to one seen at −20.1 ppm in the $^{31}P\{^1H\}$ NMR spectrum for the platinum system was seen with our catalysts as well. We have identified this species as the Markovnikov branched product, which was generated as a minor product (the ratio of anti-Markovnikov to Markovnikov product was approximately 4.5:1). The control experiment with no ruthenium complex and only KO*t*Bu was also carried out, and it was found that base itself under exactly the same reaction conditions was not an effective catalyst (less than 10% conversion after 24 h).

Scheme 7. Hydrophosphination of Acrylonitrile Catalyzed by Phosphido Complexes 2 and 7

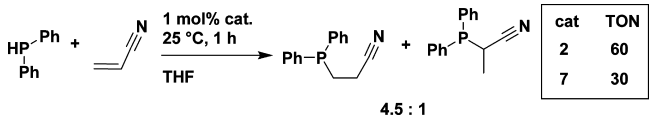

While we have not done mechanistic studies to probe the catalytic cycle, a Michael addition mechanism (Scheme 8) seems very reasonable on the basis of the pK_a values that we have determined (Table 2). Scheme 8 shows the very basic phosphido complex **7** undergoing a Michael addition reaction with acrylonitrile to generate a nitrile-stabilized carbanion. This carbanion must be more basic than deprotonated acetonitrile (pK_a^{DMSO} = 31,[90] pK_a^{THF} = 35[76]) and thus is likely to deprotonate free PPh$_2$H (pK_a^{THF} = 38; Table 2). The very

Scheme 8. Proposed Catalytic Cycle for Hydrophosphination Catalyzed by 7

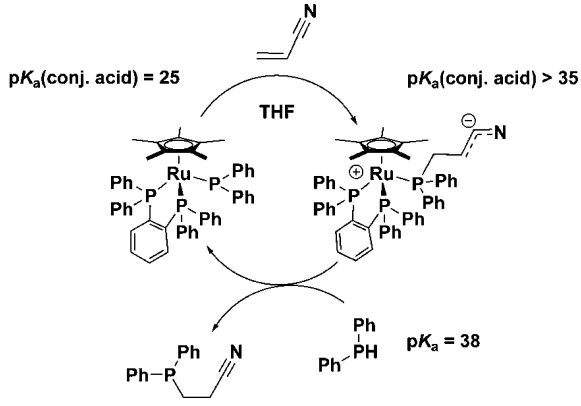

dx.doi.org/10.1021/ja5006724 | J. Am. Chem. Soc. 2014, 136, 4746−4760

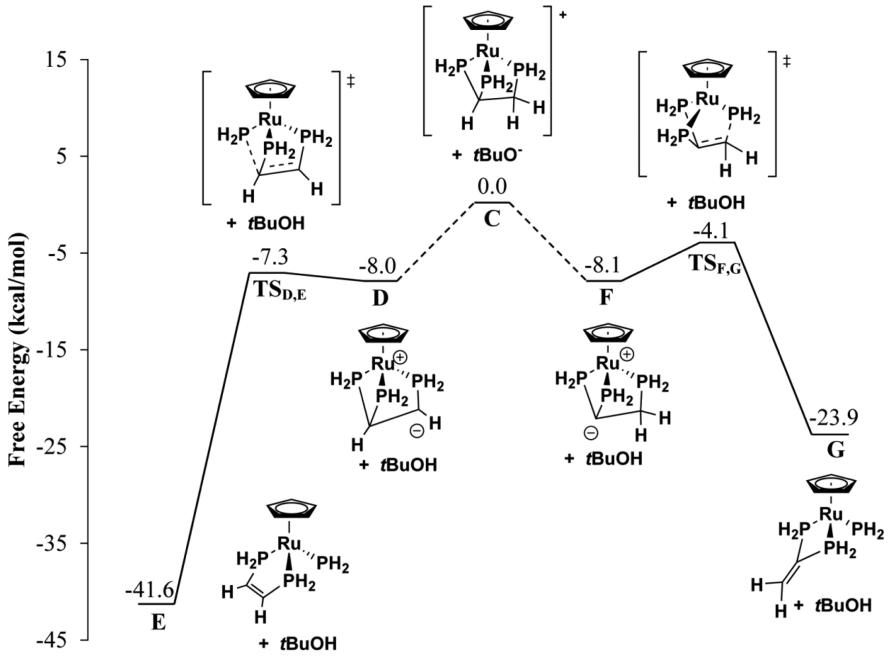

Figure 5. Free energy profile for the two possible deprotonation and fragmentation pathways of the 1,1,2-tris(diphenylphosphino)ethane complex [M06/6-31++G(d,p)/SDD-Ru/IEF-PCM + SMD(THF)]. All energies are relative to **C** + tBuO$^-$.

nucleophilic diphenylphosphide formed in this way could then displace the phosphinonitrile and coordinate to ruthenium, thus regenerating the catalyst and releasing the hydrophosphinated product.

The basicity of coordinated secondary phosphines impacts the way hydrophosphination reactions should be approached. On the basis of these NMR studies, toluene and THF should be ideal solvents, and indeed these solvents are the most popular for hydrophosphination reactions, while more acidic solvents such as MeOH and DCM should be avoided.[22,26,37,38,44,51,55−62] With respect to substrate choice for alkene hydrophosphination, activated olefins such as acrylonitrile and α,β-unsaturated enones are typically used.[22,26,37,38,44,51,55−57,59−62] For acrylonitrile, there are no acidic protons, but α,β-unsaturated enones may have acidic, enolizable protons; these should be avoided to prevent unwanted side reactions and catalyst poisoning. In fact, mainly aryl-substituted α,β-unsaturated enones are tested for late-transition-metal-catalyzed alkene hydrophosphination reactions, and this may be due to factors other than the electron-withdrawing nature of these substituents.[25,51,55−62] Lastly, when developing ligands for hydrophosphination reactions, the acidity of the ligand backbone should be considered carefully in order to preclude catalyst degradation.

DFT Calculations on the Formation of 2. Detailed computational studies utilizing density functional theory (DFT) with the model complex [Ru(η^5-C_5H_5)-((PH$_2$)$_2$CHCH$_2$PH$_2$)]$^+$ (**C**) (in which all of the phenyl and methyl groups were removed to reduce computational costs) with THF solvation were conducted in order to probe the energetics of the fragmentation of tppe upon deprotonation of complex **1** (Figure 5). The theoretical studies were based on the initial presence of **C** as well as the strong base tBuO$^-$, and therefore, all of the energies are relative to these species. From this starting point, two distinct reaction pathways were considered: (i) deprotonation at the carbon α to the lone phosphorus donor (**C** → **D**) and elimination of a phosphido to give the observed product (**D** → **E**) and (ii) deprotonation of the carbon β to the lone phosphorus donor (**C** → **F**) followed by elimination of a phosphido (**F** → **G**). Even though we took measures to minimize the errors in the energies of the starting cation and the resulting neutral species by using a solvation model, it should be kept in mind that comparing the energy of cation **C** with those of the neutral species **D** to **G** will have a greater uncertainty than comparing the energies of the neutral species.

Calculations showed that both deprotonation events were equally viable, giving ground-state structures **D** and **F** with nearly identical free energies of −8.0 and −8.1 kcal/mol, respectively. The two paths then diverged in their relative free energies, with the formation of **E** clearly shown as both the kinetic product [$\Delta G^{\circ\ddagger}_{solv}$(**TS$_{D,E}$**) = 0.7 kcal/mol] and the thermodynamic product (G°_{solv}(**E**) = −41.6 kcal/mol). The other pathway was also kinetically feasible [$\Delta G^{\circ\ddagger}_{solv}$(**TS$_{F,G}$**) = 4.0 kcal/mol], but the product, **G**, was significantly higher in free energy than **E** [G°_{solv}(**G**) = −23.9 kcal/mol]. Although both activation free energies were quite modest in the forward direction, for the back reactions they were significantly larger and differed greatly: 34.3 and 19.8 kcal/mol for **E** → **D** and **G** → **F**, respectively. It is evident that the interconversion between **E** and **D** has a large kinetic barrier, whereas the interconversion between **F** and **G** is more reasonable at ambient temperature. This likely gives the system a mechanism to equilibrate toward the thermodynamic sink and the observed product, **E**. Selected ground-state and transition-state geometries are shown in Figure 6. The elongated ruthenium−phosphido bonds in the structures of **E** and **G** should be noted.

Although the initial DFT calculations were useful for a qualitative examination of the preferential formation of **E** over **G**, they were inadequate when considering the dynamic behavior of the phosphorus moieties exemplified by the formation of **5**. The barrier between **E** and **D** (34.3 kcal/mol) was unreasonably high and did not agree with the experimental results, which showed that the phosphorus

dx.doi.org/10.1021/ja5006724 | J. Am. Chem. Soc. 2014, 136, 4746−4760

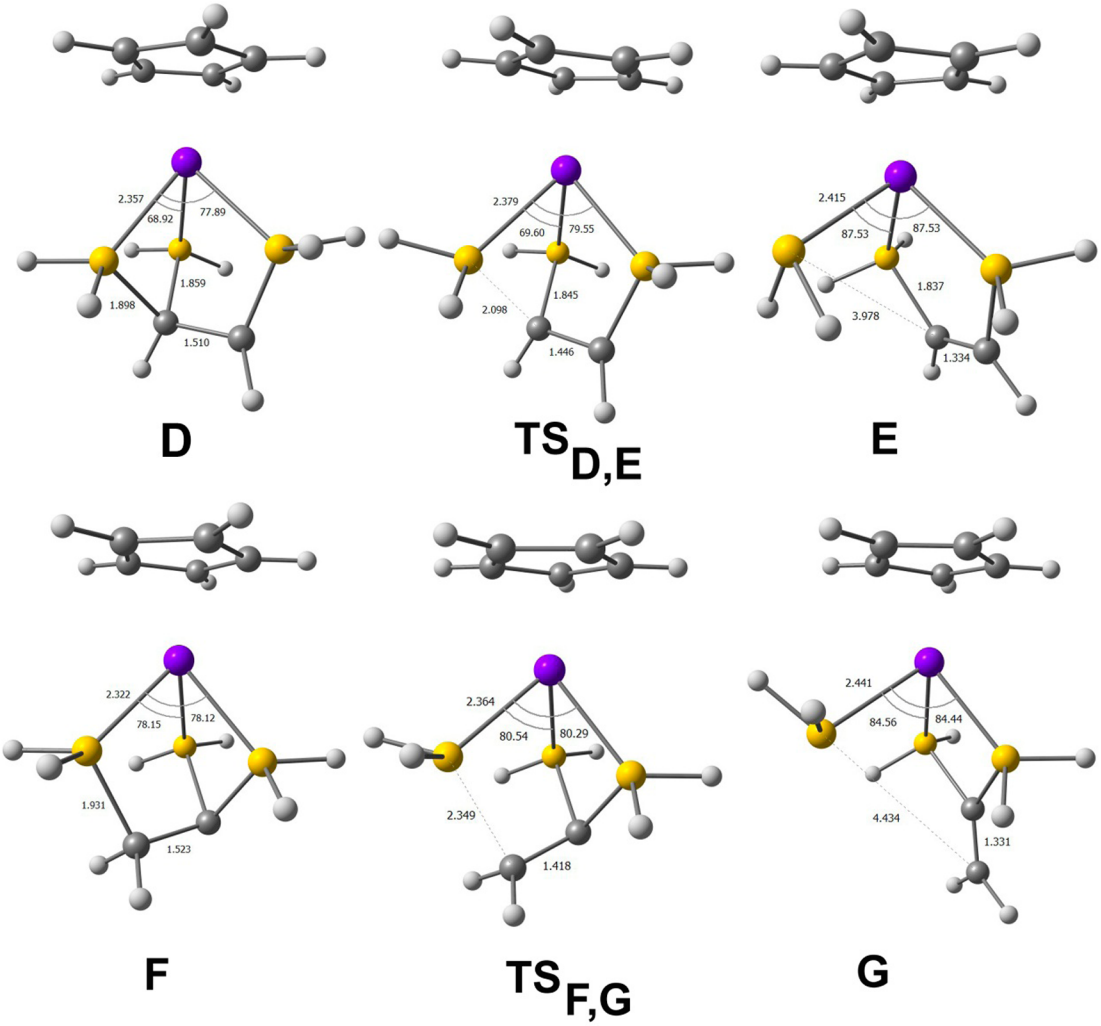

Figure 6. Optimized structures [M06/6-31++G(d,p)/SDD-Ru/IEF-PCM + SMD(THF)] as well as selected bond lengths (Å) and angles (deg) of **D**, $\mathbf{TS_{D,E}}$ (363i cm^{-1}), **E**, **F**, $\mathbf{TS_{F,G}}$ (345i cm^{-1}), and **G**.

functionalities could exchange at room temperature. It is important to note, however, that the calculations were performed on a simplified model system where the steric demands of the system were not modeled. Because the steric parameters were neglected, fragmentation of the ligand released an exaggerated amount of energy because it accounted only for the release of the ring strain imposed by the tripodal ligand architecture. Upon fragmentation of the ligand, however, the phosphorus donors move apart, which would bring the phenyl substituents closer to the methyl groups on the Cp* ligand. This would increase the steric strain of the system and help counterbalance the energy gained upon ring opening of the four-membered metallocycle.

Computational studies with the full structures of **D** and **E** ($\mathbf{D_{full}}$ and $\mathbf{E_{full}}$, respectively) were consequently conducted in order to compare the relative energies of the two species. A smaller basis set was used to reduce the computational costs, and $\mathbf{D_{full}}$ was arbitrarily selected as the reference free energy (0.0 kcal/mol). The free energy difference between $\mathbf{E_{full}}$ (−17.2 kcal/mol) and $\mathbf{D_{full}}$ was found to be 17.2 kcal/mol, which was significantly smaller than that between **E** and **D** (33.6 kcal/mol; Figure 5). This drastic decrease in the energy gap between the two species indicates that a more reasonable barrier for phosphido exchange exists and that sterics play a major role in destabilizing the product $\mathbf{E_{full}}$ in order to allow this phenomenon to take place.

This observed exchange of phosphorus moieties and outer-sphere attack of a phosphido ligand on a noncoordinated C−C double bond provides theoretical and experimental evidence for proposed steps in catalytic hydrophosphination mechanisms. These include outer-sphere attack of a phosphido ligand on a pendant alkene coordinated to the metal through a heteroatom substituent or, alternatively, a Michael addition to a free alkene. Although Michael addition mechanisms are popular in the hydrophosphination literature, in general there is very little experimental evidence to support these proposed catalytic cycles.[22−26,37,38,41,42,44,47−54,56−63] The most convincing support was provided by Glueck and co-workers, who invoked an outer-sphere Michael addition mechanism in platinum-catalyzed hydrophosphination reactions.[23,24] Our findings suggest that outer-sphere attack of a coordinated phosphido group on an activated alkene is favorable and that coordination of an alkene heteroatom substituent may be more important than initially anticipated.[46,48]

Decomposition/Rearrangement of Complex 2. Early attempts to crystallize complex **2** were conducted under N_2 at 25 °C, and after approximately 9 days, large orange crystals suitable for single-crystal XRD studies formed in excellent yield

dx.doi.org/10.1021/ja5006724 | J. Am. Chem. Soc. 2014, 136, 4746−4760

(94%). However, the product obtained was not compound **2** but a constitutional isomer, **9**, that displayed several interesting features (Scheme 9).

Scheme 9. Decomposition/Rearrangement of Complex 2 To Give Complex 9 in 94% Yield

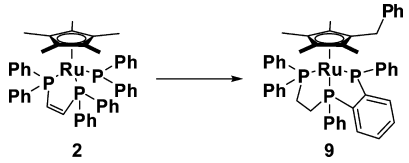

The ruthenium metal center exhibits a distorted-piano-stool geometry with a functionalized Cp* ligand opposing a *fac* tridentate diphosphinephosphido ligand (Figure 7). The Ru–P

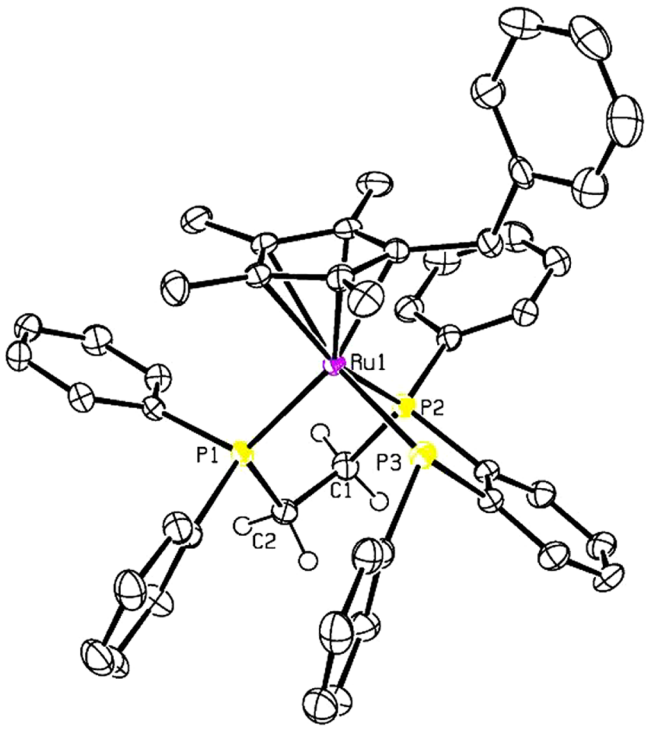

Figure 7. ORTEP3 representation and atom numbering for **9** (thermal ellipsoids at 50% probability; most of the hydrogens omitted for clarity).

bond lengths for the phosphine donors, Ru(1)–P(1) and Ru(1)–P(2), are similar to those seen for complex **2** [2.269(2) and 2.254(2) Å, respectively], while the phosphido donor displays an elongated Ru(1)–P(3) bond length of 2.366(2) Å (attributed to the gauche effect). It is also evident from the crystal structure that the new tridentate ligand constrains the geometry about the metal center and contracts two of the P–Ru–P bond angles, P(1)–Ru(1)–P(2) and P(2)–Ru(1)–P(3), below the optimal octahedral angle of 90° [83.83(6) and 83.77(6)°, respectively]. The P(1)–Ru(1)–P(3) angle, on the other hand, is obtuse (99.53°) and is likely pulled open by the two five-membered rings linking the three phosphorus donors (see Table 1 for other notable bond lengths and angles).

The rearrangement product **9** was characterized not only by XRD but also by NMR spectroscopy. The $^{31}P\{^{1}H\}$ NMR spectrum showed a very diagnostic pattern of two sets of doublets of doublets and a broad singlet for the three inequivalent phosphorus nuclei. The two phosphine donors exhibited peaks at 99.8 and 86.5 ppm, while the phosphido peak was shifted upfield to around 66.4 ppm. The ^{1}H NMR spectrum was also very revealing. Four inequivalent methyl peaks were evident at 1.54, 1.46, 1.41, and 1.35 ppm, indicating that functionalization of the Cp* ligand had occurred and that all symmetry in the molecule was lost. Moreover, a methylene peak at around 3.1 ppm for benzylic protons also confirmed that activation of the Cp* had taken place, whereas two sets of overlapping methylene peaks at around 2.2 ppm showed that the unsaturated backbone of the dppen ligand had been reduced.

It is interesting to note that all atoms are conserved upon conversion of **2** to **9** and that this process proceeds even in the dark, demonstrating that it is not a photochemical reaction (Scheme 9). In order to generate the rearranged species, several key transformations need to occur. First, activation of a Cp* methyl group and migration of a phenyl functionality from a phosphorus center is necessary to produce the 1-benzyl-2,3,4,5-tetramethylcyclopentadienyl ligand. It is known in the literature that tetramethylfulvene is susceptible to nucleophilic attack, and Maitlis and co-workers have shown that even a chloride ligand can migrate to tetramethylfulvene to produce a functionalized Cp* on ruthenium.[91−96] Furthermore, reports indicate that the electronic structure of "tucked-in" complexes can be viewed as either tetramethylfulvene and M^{n+} or a tetramethylfulvenide ligand and $M^{(n+2)+}$, but regardless, it is known that this ligand can be converted to a functionalized Cp* ligand, whether through reductive elimination or intramolecular nucleophilic attack.[97−110] To generate the tridentate (2-((2-(diphenylphosphino)ethyl)(phenyl)phosphino)phenyl)-(phenyl)phosphido ligand, three key steps need to take place: P–C bond cleavage and elimination of a phenyl group, as mentioned previously; activation of an aromatic *o*-C–H bond and coupling to a phosphorus center; and hydrogenation of the unsaturated dppen backbone. The Rosenberg and Peters groups have both shown that phosphidos are able to deprotonate and orthometalate a phenyl substituent of a *cis*-phosphine ligand on coordinatively unsaturated ruthenium(II) complexes.[17,28,36] This, followed by deprotonation of the resulting phosphine and reductive elimination of the alkyl and phosphido functionalities, could form the 1,2-diphosphinobenzene linkage. In order to reduce the unsaturated backbone from the dppen ligand, on the other hand, the hydrogen atoms would need to come from the activated Cp* methyl group and the aromatic *o*-C–H bond. Attack by a hydride on the alkene and subsequent protonation of the corresponding alkyl species by a phosphine could yield the ethylidene fragment (see Table 3 for possible elements of the rearrangement mechanism).

Attempts were made to probe the formation of complex **9** utilizing both $^{31}P\{^{1}H\}$ and ^{1}H NMR spectroscopy, with an emphasis on identifying hydride peaks in the ^{1}H NMR spectrum. A small amount of complex **2** was dissolved in toluene-d_8, placed in a J-Young tube, and layered with pentane (the addition of pentane was important for isolating the crystalline product, which decomposed over time when dissolved in solution). Then, over the course of 13 days, the pentane was allowed to slowly diffuse into the toluene solution and NMR spectra were taken periodically (see Figure S1 in the Supporting Information). After 2 days, three peaks appeared in the $^{31}P\{^{1}H\}$ NMR spectrum: two doublets of doublets at 99.8

dx.doi.org/10.1021/ja5006724 | J. Am. Chem. Soc. 2014, 136, 4746−4760

Table 3. Possible Steps of the Rearrangement Mechanism of the Reaction in Scheme 9 and Similar Reactions Found in the Literature[a]

Transformation	Example from Literature	Reference(s)
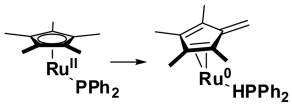	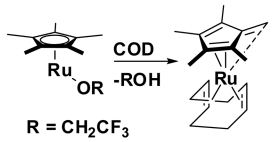	92,111,112
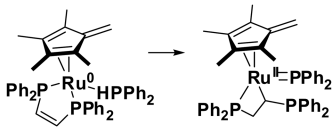	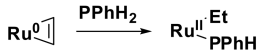	113
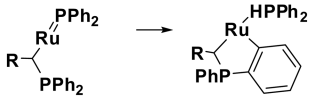	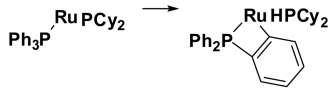	17,28,36
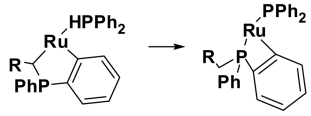	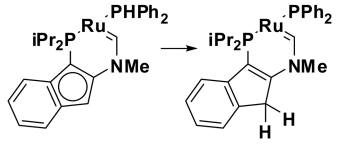	75
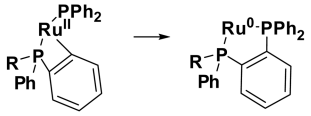	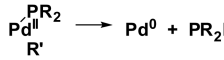	54,55
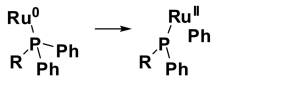	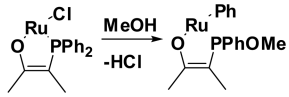	114-120
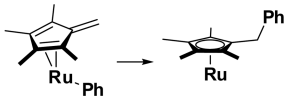	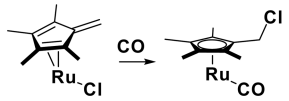	91-96

[a]It should be noted that this table simply displays a series of reactions that could be involved in the formation of **9**, and the order in which they are presented is not meant to be taken as a definitive sequence of events that must be followed.

and 86.5 ppm as well as a broad singlet at around 66.4 ppm. These peaks corresponded to the product **9**. Over the next 5 days, the concentration of **9** in solution increased until crystals began to form in the NMR tube on day 8. The signals for **9** then slowly disappeared over 6 days, while more of the rearrangement product crystallized out of solution. Throughout the entire study, no hydrides could be detected in the ^{1}H NMR spectra.

After failing to glean any significant mechanistic insight from the ^{31}P{^{1}H} and ^{1}H NMR study of the formation of **9**, the synthesis of **5** was pursued. It was thought that incorporation of a bis(*p*-tolyl)phosphido ligand would provide a way to determine which aromatic group is transferred to the Cp* moiety and which substituent on phosphorus is activated at the ortho position. Unfortunately, the migratory nature of the phosphorus donors in the dppen phosphido species revealed that complex **5** could not be used for its intended purpose. If a phenyl or *p*-tolyl group were transferred to the Cp* ligand during the rearrangement process, there would be no way to confidently conclude whether it originated from the bidentate ligand or the phosphido moiety. Essentially, because the different phosphorus functionalities can exchange, deuterating or functionalizing any of their substituents would provide no reliable mechanistic information on the formation of **9**. Therefore, mechanistic studies on the rearrangement reaction have reached an impasse.

Currently it is premature to propose a mechanism for the formation of the rearrangement product because of a lack of evidence for any intermediates and because of the many steps that need to take place in going from complex **2** to complex **9**. What can be proposed with a degree of certainty is that the first step in the rearrangement process is rate-limiting and is followed by a series of fast low-barrier transformations. This may also explain why the yield is so high and the reaction is so selective: after the initial slow step, the transient intermediates form the product so quickly that they are not intercepted by any other reactants.

Although the rearrangement reaction that produces **9** may not be broadly applicable to other systems, it does illustrate the high reactivity of the phosphido ligands and the unpredictability of their transformations. The example of **9** is likely an extreme case of how a phosphido ligand can facilitate unexpected ligand rearrangements, but its formation demonstrates how carefully ancillary ligands must be chosen for metal centers bearing

dx.doi.org/10.1021/ja5006724 | J. Am. Chem. Soc. 2014, 136, 4746−4760

phosphido moieties. It is possible that the best ligands for catalytic hydrophosphination are those that not only provide the correct stereoelectronic environment to facilitate the reaction but also are robust enough to withstand the phosphido intermediates. It is also important to note that many ligands that are traditionally thought to be stable, such as Cp* and triphenylphosphine, may not be robust enough under these conditions.

CONCLUSIONS

We have described the base-promoted dehydrophosphination of the tppe ligand in **1** to generate a ruthenium dppen phosphido complex **2** and explored the reactivity of the deprotonated species in the context of alkene hydrophosphination reactions and mechanisms. It was found that the pK_a of the phosphido ligands was important in dictating the stability of the metal complexes, to the extent that the more electron-rich bis(*p*-tolyl)phosphido functionality exchanged with a diphenylphosphino moiety of the dppen ligand to generate the more stable species **5**. This has implications for hydrophosphination reactions, where the electron richness of the phosphido ligand has to be managed carefully in order to prevent unwanted swapping of phosphorus groups during the synthesis of chiral, multidentate phosphorus ligands. Furthermore, the measured pK_a values of the phosphido complexes were used to rationalize a possible catalytic mechanism for complexes **2** and **7**, which were capable of effecting the addition of diphenylphosphine to acrylonitrile. Moreover, the pK_a studies illustrated that the acidity of the solvent, substrates, and ligand backbones have to be carefully considered in these reactions. DFT studies of the tppe fragmentation and the exchange of phosphorus moieties were also enlightening in that they showed that an outer-sphere attack of a phosphido ligand on a pendant alkene coordinated to the metal through a heteroatom is energetically accessible at room temperature. This gives support for Michael addition mechanisms for the hydrophosphination of alkenes, which are popular in the hydrophosphination literature. Lastly, the unexpected reactivity of phosphido ligands was highlighted by an unprecedented rearrangement reaction in which P−C, C−C, and C−H bonds were made and broken to produce **9**, a constitutional isomer of **2**. The rearrangement reaction stresses the importance of designing robust ligands for hydrophosphination reactions and shows that ligands that are traditionally considered "stable" may undergo unpredictable decomposition pathways under relatively mild conditions.

EXPERIMENTAL SECTION

General Considerations. Procedures and manipulations were performed under an argon or nitrogen atmosphere using standard Schlenk line and glovebox techniques, unless stated otherwise. Solvents were degassed and dried using standard procedures prior to all manipulations and reactions, unless stated otherwise. The synthesis of complex **1** was described previously,[64] as was the synthesis of RuCp*(cod)Cl.[121] The 1-*tert*-butyl-2,2,4,4,4-pentakis(dimethylamino)-2λ^5,4λ^5-catenadi(phosphazenium) tetrafluoroborate salt was synthesized from commercially available 1-*tert*-butyl-2,2,4,4,4-pentakis(dimethylamino)-2λ^5,4λ^5-catenadi(phosphazene) and tetrafluoroboric acid diethyl ether complex (purchased from Sigma-Aldrich and used without further purification). Deuterated solvents were purchased from Cambridge Isotope Laboratories or Sigma-Aldrich, degassed, and dried over activated molecular sieves prior to use. All other reagents were purchased from commercial sources and utilized without further purification. The electrospray ionization mass spectrometry (ESI-MS) data were collected on an AB/Sciex QStar mass spectrometer with an ESI source. The electron impact mass spectrometry (EI-MS) data were collected on a Waters GC ToF mass spectrometer with an EI/CI source, and the direct analysis in real time mass spectrometry (DART-MS) data were collected on a JEOL AccuTOF-DART mass spectrometer with a DART ion source (no solvent is required). NMR spectra were recorded at ambient temperature and pressure using a Varian Gemini 400 MHz spectrometer (400 MHz for ^{1}H, 100 MHz for ^{13}C, 376 MHz for ^{19}F, and 161 MHz for ^{31}P) or an Agilent DD2 600 MHz spectrometer (600 MHz for ^{1}H, 151 MHz for ^{13}C, 564 MHz for ^{19}F, and 243 MHz for ^{31}P), unless stated otherwise. The ^{1}H and ^{13}C NMR chemical shifts were measured relative to partially deuterated solvent peaks but are reported relative to tetramethylsilane (TMS). All of the ^{31}P chemical shifts were measured relative to 85% phosphoric acid as an external reference. The elemental analyses were performed at the Department of Chemistry, University of Toronto, on a PerkinElmer 2400 CHN elemental analyzer. Single-crystal XRD data were collected using a Nonius Kappa-CCD or Bruker Kappa APEX DUO diffractometer with Mo Kα radiation (λ = 0.710 Å) or Cu Kα radiation (λ = 2.29 Å). The CCD data were integrated and scaled using the Denzo-SMN package. The structures were solved and refined using SHELXTL version 6.1. Refinement was by full-matrix least-squares on F^2 using all data. For compounds where extra solvent was evident in the elemental analysis, there was evidence for the additional solvent either in the XRD structure (solvent was seen or was removed using the SQUEEZE function) or in the NMR spectra of the purified compounds.

Computational Details. DFT calculations were performed using the Gaussian 09 package[122] and the M06 hybrid functional.[123−125] Ruthenium was treated with the SDD relativistic effective core potential and associated basis set,[126,127] while all other atoms were treated with the 6-31++G(d,p) or 6-31+G(d) basis set.[128−130] A pruned (99,590) integration grid was used throughout (Grid=-UltraFine). The substituents on phosphorus and Cp* were replaced with hydrogen atoms to reduce the computational cost, except where stated otherwise. Optimizations were performed using the integral equation formalism polarizable continuum model (IEF-PCM)[131,132] with radii and nonelectrostatic terms from the SMD solvation model for THF.[133] Ground states were connected to their transition states by performing intrinsic reaction coordinate (IRC) calculations.[134] Odd-electron species were not considered, and stationary points were characterized by normal-mode analysis. Full vibrational and thermochemical analyses (1 atm, 298 K) were performed on optimized structures to obtain solvent-corrected free energies ($G°$) and enthalpies ($H°$). Optimized ground states were found to have zero imaginary frequencies, while transition states were found to have one imaginary frequency. Three-dimensional visualizations of calculated structures and molecular orbitals were generated by ChemCraft.

Determination of pK_a in THF. Equilibrium constants were determined using gated−decoupled ^{31}P NMR spectroscopy (in nondeuterated THF). The experimentally determined T_1 values were all less than 10 s on a Varian Gemini 400 MHz spectrometer, and thus, the recycling time (D1 + AT) was set to 2.363 s and a 30° pulse was employed (the Ernst equation gives a maximum angle of 37.9° for this D1 + AT, indicating that the signals will be completely relaxed and integrations will be quantitative in this field).[135] To determine the pK_a of bis(*p*-tolyl)phosphine, 1 equiv of diphenylamine was completely deprotonated with KH in the presence of 4,7,13,16,21,24-hexaoxa-1,10-diazabicyclo[8.8.8]hexacosane (2.2.2-cryptand), and a solution of bis(*p*-tolyl)phosphine was added. Three independent reactions with varying concentrations of bis(*p*-tolyl)-phosphine were utilized to calculate the reported pK_a value (see the Supporting Information for sample calculations). For the metal complexes, the experimentally determined T_1 values were all less than 16 s on a Agilent DD2 600 MHz spectrometer, and thus, the recycling time (D1 + AT) was set to 2.891 s and a 30° pulse was employed in order to obtain quantitative integrations.[135] To determine the pK_a of **7**, the ruthenium complex was dissolved in THF, and a solution of 1-*tert*-butyl-2,2,4,4,4-pentakis(dimethylamino)-2λ^5,4λ^5-catenadi-(phosphazenium) tetrafluoroborate salt was added. Three independent

dx.doi.org/10.1021/ja5006724 | J. Am. Chem. Soc. 2014, 136, 4746−4760

reactions with varying concentrations of ruthenium complex and phosphazenium salt were utilized to calculate the reported pK_a value. The pK_a of **8** was determined in a similar fashion using three independent reactions with varying concentrations of ruthenium complex and phosphazenium salt as well. The values are listed in Table 2. To reduce sources of error, the amount of solvent added was determined by weight.

Synthesis of RuCp*(Ph$_2$PCHCHPPh$_2$)(PPh$_2$) (2). A small amount of **1** (0.020 g, 0.021 mmol) was dissolved in THF (2 mL). An excess of KO*t*Bu (0.010 g, 0.089 mmol) was added. The resulting deep-red solution was evaporated to dryness and dissolved in toluene (2 mL). The solution was left in the freezer at −33 °C overnight and then filtered. The solvent was removed under reduced pressure to give a brick-red powder. Yield: 94% (0.016 g). Crystals suitable for XRD studies were grown by slow diffusion of pentane into a toluene solution of the complex at −33 °C. ^{1}H NMR (400 MHz, THF-d_8) δ: 7.66−7.57 (m, 4H, Ar−CH), 7.43−7.35 (m, 5H, Ar−CH and CH═CH), 7.24−7.17 (m, 3H, Ar−CH and CH═CH), 7.13−7.06 (m, 6H, Ar−CH), 6.89 (t, 4H, J = 8.4 Hz), 6.67 (t, 2H, Ar−CH, J = 7.2 Hz), 6.52 (t, 4H, Ar−CH, J = 7.5 Hz), 6.44−6.36 (m, 4H, Ar−CH), and 1.12 (s, 15H, Cp*−CH$_3$) ppm. ^{31}P{^{1}H} NMR (161 MHz, THF-d_8) δ: 79.22 (d, J = 8.1 Hz) and 23.21 (t, J = 8.1 Hz) ppm. ^{13}C{^{1}H} NMR (100 MHz, THF-d_8) δ: 148.18 (d, C−P, J = 44.6 Hz), 146.92 (dd, CH−P, J = 38.4, 32.7 Hz), 139.31 (d, C−P, J = 38.4 Hz), 136.81 (d, C−P, J = 44.6 Hz), 136.55 (d, Ar−CH, J = 19.5 Hz), 133.97 (q, Ar−CH, J = 5.1 Hz), 133.21 (dd, Ar−CH, J = 5.2 Hz), 129.03 (s, Ar−CH), 128.48 (s, Ar−CH), 127.60 (dd, Ar−CH, J = 4.6 Hz), 126.82 (dd, Ar−CH, J = 4.4 Hz), 125.19 (d, Ar−CH, J = 5.4 Hz), 123.47 (s, Ar−CH), 93.05 (t, Cp*-C, J = 2.0 Hz), and 9.60 (d, Cp*−CH$_3$, J = 5.3 Hz) ppm. Anal. Calcd for [$C_{48}H_{47}P_3Ru$]·0.50C_7H_8: C, 71.60; H, 5.95. Found: C, 71.22; H, 6.34. MS (DART, no solvent; m/z^+): 819.0 [$C_{48}H_{48}P_3Ru$]$^+$.

Synthesis of [RuCp*(Ph$_2$PCHCHPPh$_2$)(HPPh$_2$)][HCl$_2$] (3). A small amount of **2** (0.030 g, 0.037 mmol) was dissolved in toluene (2 mL), and an excess of 1 M HCl/ether (0.08 mL, 0.080 mmol) was added. The solution turned from red to pale yellow, and a yellow precipitate formed. The resulting yellow powder was isolated by filtration and washed with small amounts of ether (1 mL) and pentane (2 mL). Yield: 76.5% (0.025 g). Crystals suitable for XRD studies were grown by slow diffusion of pentane into a DCM solution of the complex. ^{1}H NMR (400 MHz, CD_2Cl_2) δ: 7.73−7.65 (m, 6H, Ar−CH), 7.65−7.57 (m, 5H, Ar−CH and P−CH), 7.45 (d, 1H, P−CH, J = 24.1 Hz), 7.42 (t, 2H, Ar−CH, J = 7.0 Hz), 7.31 (td, 4H, Ar−CH, J = 7.6 Hz), 7.14 (t, 2H, Ar−CH, J = 7.0 Hz), 6.98−6.90 (m, 6H, Ar−CH), 6.46 (dd, 4H, Ar−CH, J = 11.4, 7.2 Hz), 6.05 (dt, 1H, PH, J = 356.7, 5.6 Hz), and 1.44−1.41 (m, 15H, Cp*−CH$_3$) ppm. ^{31}P{^{1}H} NMR (161 MHz, CD_2Cl_2) δ: 74.61 (d, J = 35.8 Hz) and 37.92 (t, J = 35.8 Hz) ppm. ^{13}C{^{1}H} NMR (100 MHz, CD_2Cl_2) δ: 146.22 (dd, P−CH, J = 35.5, 32.6 Hz), 134.35 (dd, C−P, J = 42.5, 2.9 Hz), 133.87 (dd, C−P, J = 48.8, 3.5 Hz), 132.58 (t, Ar−CH, J = 5.4 Hz), 132.48 (d, Ar−CH, J = 10.3 Hz), 132.32 (d, Ar−CH, J = 9.0 Hz), 131.91 (d, C−P, J = 42.4 Hz), 131.56 (s, Ar−CH), 130.64 (s, Ar−CH), 129.57 (t, Ar−CH, J = 4.9 Hz), 129.56 (s, Ar−CH), 128.23 (t, Ar−CH, J = 4.9 Hz), 128.11 (d, Ar−CH, J = 9.5 Hz), and 9.72 (s, Cp*−CH$_3$) ppm. Anal. Calcd for [$C_{48}H_{47}P_3Ru$][Cl_2H]·0.25CH_2Cl_2: C, 63.54; H, 5.47. Found: C, 63.54; H, 5.91. MS (ESI$^+$, DCM; m/z^+): 819.2 [$C_{48}H_{47}P_3Ru$]$^+$.

Synthesis of RuCp*(Ph$_2$PCHCHPPh$_2$)Cl (4). Both *cis*-1,2-bis(diphenylphosphino)ethene (0.104 g, 0.26 mmol) and RuCp*(cod)Cl (0.100 g, 0.26 mmol) were dissolved in dichloromethane (DCM) (10 mL), and the solution was heated at 36 °C overnight. The solvent was removed under reduced pressure, and the resulting orange solid was washed with hexanes. Yield: 83% (0.147 g). ^{1}H NMR (400 MHz, CD_2Cl_2) δ: 7.73−7.62 (m, 4H, Ar−CH), 7.50 (d, 2H, P−CH, J = 58.5 Hz), 7.44−7.38 (m, 6H, Ar−CH), 7.38−7.26 (m, 6H, Ar−CH), 7.12 (t, 4H, Ar−CH, J = 8.4 Hz), and 1.44 (s, 15H, Cp*−CH$_3$) ppm. ^{31}P{^{1}H} NMR (161 MHz, CD_2Cl_2) δ: 81.14 (s) ppm. ^{13}C{^{1}H} NMR (100 MHz, CD_2Cl_2) δ: 147.52 (dd, P−CH, J = 34.6, 33.5 Hz), 137.86 (dd, C−P, J = 43.5, 4.5 Hz), 133.93 (t, Ar−CH, J = 5.2 Hz), 133.07 (dd, C−P, J = 45.4, 2.2 Hz), 132.53 (t, Ar−CH, J = 5.3 Hz), 129.28 (s, Ar−CH), 129.16 (s, Ar−CH), 127.70 (t, Ar−CH, J = 4.5 Hz), 127.51 (t, Ar−CH, J = 4.8 Hz), 89.64 (t, Cp*-C, J = 2.6 Hz), and 9.51 (s, Cp*−CH$_3$) ppm. Anal. Calcd for [$C_{36}H_{37}ClP_2Ru$]·0.50CH_2Cl_2: C, 61.69; H, 5.39. Found: C, 61.88; H, 5.32. MS (ESI$^+$, DCM; m/z^+): 668.1 [$C_{36}H_{38}ClP_2Ru$]$^+$.

Alternative Synthesis of Complex 2. A small amount of **4** (0.031, 0.046 mmol) was dissolved in THF (2 mL), and AgOTf (0.011 g, 0.046 mmol) in THF (1 mL) was added. The solution turned orange with a dark-gray precipitate. The mixture was stirred for 30 min in the dark and then filtered. A solution of diphenylphosphine (0.009 g, 0.046 mmol) in THF (2 mL) was added to the filtrate, and the solution turned from orange to yellow in color. The reaction mixture was stirred for an additional 30 min, and KO*t*Bu (0.005 g, 0.046 mmol) in THF (1 mL) was added. The solution immediately turned dark red in color. The solvent was removed under reduced pressure, and the red residue was redissolved in toluene (∼2 mL). The solution was cooled to −33 °C in a freezer overnight and then filtered through Celite. Hexanes (∼4 mL) was added, and the solution was once again cooled to −33 °C in a freezer overnight. The red precipitate was collected and washed with hexanes (∼2 mL) to give a brick-red powder. Yield: 53% (0.020 g). All of the spectroscopic data were identical to those of **2**.

Synthesis of RuCp*(Ph$_2$PCHCHP(*p*-tol)$_2$)(PPh$_2$) (5). This was similar to the alternative synthesis of **2** (see p S2 in the Supporting Information).

Synthesis of RuCp*(Ph$_2$PC$_6$H$_4$PPh$_2$)Cl (6). This was similar to the synthesis of **4** (see pp S2−S3 in the Supporting Information).

Synthesis of RuCp*(Ph$_2$PC$_6$H$_4$PPh$_2$)(PPh$_2$) (7). This was similar to the alternative synthesis of **2** (see p S3 in the Supporting Information).

Synthesis of RuCp*(Ph$_2$PC$_6$H$_4$PPh$_2$)(P(*p*-tol)$_2$) (8). This was similar to the alternative synthesis of **2** (see pp S3−S4 in the Supporting Information).

Synthesis of Ru(C$_5$(CH$_3$)$_4$(CH$_2$C$_6$H$_5$))(Ph$_2$PCH$_2$CH$_2$PPh(*o*-C$_6$H$_4$)PPh) (9). A small amount of **2** (0.010 g, 0.012 mmol) was dissolved in toluene (∼1 mL), and a large amount of pentane (∼3 mL) was slowly diffused into the solution over 9−10 days. The resulting orange crystals were filtered and dried under reduced pressure. Yield: 93% (0.09 g). Crystals suitable for XRD studies were grown by diffusion of pentane into a toluene solution of **1** after 9−10 days. ^{1}H NMR (600 MHz, THF-d_8) δ: 7.69−7.63 (m, 2H, Ar−CH), 7.58−7.52 (m, 2H, Ar−CH), 7.51−7.46 (m, 1H, Ar−CH), 7.42 (d, 1H, Ar−CH, J = 7.4 Hz), 7.28 (t, 1H, Ar−CH, J = 7.4 Hz), 7.26−7.23 (m, 2H, Ar−CH), 7.12−7.05 (m, 4H, Ar−CH), 7.03−6.94 (m, 9H, Ar−CH), 6.89−6.85 (m, 2H, Ar−CH), 6.82 (t, 2H, Ar−CH, J = 6.9 Hz), 6.61 (t, 1H, Ar−CH, J = 7.3 Hz), 6.46 (t, 2H, Ar−CH, J = 7.6 Hz), 3.14−3.04 (m, 2H, CH$_2$), 2.31−2.16 (m, 4H, CH$_2$), 1.54 (s, 3H, Cp*−CH$_3$), 1.46 (s, 3H, Cp*−CH$_3$), 1.41 (s, 3H, Cp*−CH$_3$), and 1.35 (s, 3H, Cp*−CH$_3$) ppm. ^{31}P{^{1}H} NMR (243 MHz, THF-d_8) δ: 99.79 (dd, J = 23.3, 6.5 Hz), 86.51 (dd, J = 23.3, 7.1 Hz), and 66.74−66.38 (br s) ppm. ^{13}C{^{1}H} NMR (151 MHz, THF-d_8) δ: 133.06 (d, Ar−CH, J = 21.1 Hz), 132.15 (d, Ar−CH, J = 10.4 Hz), 132.00 (d, Ar−CH, J = 8.5 Hz), 131.88−131.70 (m, Ar−CH), 129.27−129.18 (m, Ar−CH), 128.91 (d, Ar−CH, J = 1.9 Hz), 128.42 (d, Ar−CH, J = 2.2 Hz), 128.00 (d, Ar−CH, J = 1.0 Hz), 127.96−127.85 (m, Ar−CH), 127.47 (d, Ar−CH, J = 9.1 Hz), 127.02 (d, Ar−CH, J = 8.6 Hz), 126.25 (d, Ar−CH, J = 6.4 Hz), 125.04 (s, Ar−CH), 123.92−123.81 (m, Ar−CH), 94.28−93.92 (m, Cp*-C), 93.75−93.62 (m, Cp*-C), 31.02−31.0 (m, P−CH$_2$), 30.04−30.02 (m, CH$_2$), 9.92 (s, Cp*−CH$_3$), 9.84 (s, Cp*−CH$_3$), 9.79 (s, Cp*−CH$_3$), and 9.69 (s, Cp*−CH$_3$) ppm. Anal. Calcd for [$C_{48}H_{47}P_3Ru$]: C, 70.49; H, 5.79. Found: C, 70.97; H, 6.17. MS (DART, no solvent; m/z^+): 819.0 [$C_{48}H_{48}P_3Ru$]$^+$.

Hydrophosphination of Acrylonitrile. A small amount of **2** (0.005 g, 0.006 mmol) or **7** (0.005 g, 0.006 mmol) was dissolved in 1 mL of THF. A solution of diphenylphosphine (0.105 g, 0.565 mmol) in 1 mL of THF and a solution of acrylonitrile (0.031 g, 0.565 mmol) in 1 mL of THF were simultaneously added. The reaction mixture was stirred for 1 h, and conversion was determined by ^{31}P{^{1}H} NMR analysis.

dx.doi.org/10.1021/ja5006724 | *J. Am. Chem. Soc.* 2014, 136, 4746−4760

■ ASSOCIATED CONTENT

Supporting Information

Extended experimental section; complete ref 122; ^{31}P NMR spectroscopic study of the formation of **5**; sample calculations for the determination of pK_a values; crystallographic data tables for **2**, **3**, **5**, **7**, and **9** (including CIF files); and tables giving Cartesian coordinates and free energies for optimized structures. This material is available free of charge via the Internet at http://pubs.acs.org.

■ AUTHOR INFORMATION

Corresponding Author

rmorris@chem.utoronto.ca

Notes

The authors declare no competing financial interest.

■ ACKNOWLEDGMENTS

We thank NSERC Canada for a Discovery Grant to R.H.M and Demyan Prokopchuk for fruitful discussions.

■ REFERENCES

(1) Rosenberg, L. *Coord. Chem. Rev.* **2012**, *256*, 606.
(2) Miyake, Y.; Endo, S.; Yuki, M.; Tanabe, Y.; Nishibayashi, Y. *Organometallics* **2008**, *27*, 6039.
(3) Cauzzi, D.; Graiff, C.; Massera, C.; Predieri, G.; Tiripicchio, A. *Eur. J. Inorg. Chem.* **2001**, 721.
(4) Alvarez, C. M.; Garcia, M. E.; Ruiz, M. A.; Connelly, N. G. *Organometallics* **2004**, *23*, 4750.
(5) Wong, W.-Y.; Ting, F.-L.; Lin, Z. *Organometallics* **2003**, *22*, 5100.
(6) Baldovino-Pantaleon, O.; Rios-Moreno, G.; Toscano, R. A.; Morales-Morales, D. *J. Organomet. Chem.* **2005**, *690*, 2880.
(7) Dick, D. G.; Hou, Z.; Stephan, D. W. *Organometallics* **1992**, *11*, 2378.
(8) Cabeza, J. A.; Mulla, F.; Riera, V. *J. Organomet. Chem.* **1994**, *470*, 173.
(9) Süss-Fink, G.; Godefroy, I.; Beguin, A.; Rheinwald, G.; Neels, A.; Stoeckli-Evans, H. *J. Chem. Soc., Dalton Trans.* **1998**, 2211.
(10) Jungbluth, H.; Stoeckli-Evans, H.; Süss-Fink, G. *J. Organomet. Chem.* **1990**, *391*, 109.
(11) Bottcher, H.-C.; Graf, M.; Merzweiler, K.; Bruhn, C. *Polyhedron* **1998**, *17*, 3433.
(12) Eichele, K.; Wasylishen, R. E.; Corrigan, J. F.; Taylor, N. J.; Carty, A. J.; Feindel, K. W.; Bernard, G. M. *J. Am. Chem. Soc.* **2002**, *124*, 1541.
(13) Bader, A.; Nullmeyers, T.; Pabel, M.; Salem, G.; Willis, A. C.; Wild, S. B. *Inorg. Chem.* **1995**, *34*, 384.
(14) Buhro, W. E.; Zwick, B. D.; Georgiou, S.; Hutchinson, J. P.; Gladysz, J. A. *J. Am. Chem. Soc.* **1988**, *110*, 2427.
(15) Fryzuk, M. D.; Bhangu, K. *J. Am. Chem. Soc.* **1988**, *110*, 961.
(16) Gloaguen, Y.; Jacobs, W.; de Bruin, B.; Lutz, M.; van der Vlugt, J. I. *Inorg. Chem.* **2013**, *52*, 1682.
(17) Hoyle, M.-A. M.; Pantazis, D. A.; Burton, H. M.; McDonald, R.; Rosenberg, L. *Organometallics* **2011**, *30*, 6458.
(18) Planas, J. G.; Hampel, F.; Gladysz, J. A. *Chem.—Eur. J.* **2005**, *11*, 1402.
(19) Boni, G.; Blacque, O.; Sauvageot, P.; Poujaud, N.; Moise, C.; Kubicki, M. M. *Polyhedron* **2002**, *21*, 371.
(20) Fryzuk, M. D.; Joshi, K.; Chadha, R. K.; Rettig, S. J. *J. Am. Chem. Soc.* **1991**, *113*, 8724.
(21) Planas, J. G.; Gladysz, J. A. *Inorg. Chem.* **2002**, *41*, 6947.
(22) Glueck, D. S. *Synlett* **2007**, 2627.
(23) Scriban, C.; Glueck, D. S.; Zakharov, L. N.; Kassel, W. S.; DiPasquale, A. G.; Golen, J. A.; Rheingold, A. L. *Organometallics* **2006**, *25*, 5757.
(24) Scriban, C.; Kovacik, I.; Glueck, D. S. *Organometallics* **2005**, *24*, 4871.
(25) Glueck, D. S. *Top. Organomet. Chem.* **2010**, *31*, 65.
(26) Kovacik, I.; Scriban, C.; Glueck, D. S. *Organometallics* **2006**, *25*, 536.
(27) Derrah, E. J.; Pantazis, D. A.; McDonald, R.; Rosenberg, L. *Angew. Chem., Int. Ed.* **2010**, *49*, 3367.
(28) Derrah, E. J.; Pantazis, D. A.; McDonald, R.; Rosenberg, L. *Organometallics* **2007**, *26*, 1473.
(29) Derrah, E. J.; McDonald, R.; Rosenberg, L. *Chem. Commun.* **2010**, *46*, 4592.
(30) Derrah, E. J.; Giesbrecht, K. E.; McDonald, R.; Rosenberg, L. *Organometallics* **2008**, *27*, 5025.
(31) Vaughan, G. A.; Hillhouse, G. L.; Rheingold, A. L. *Organometallics* **1989**, *8*, 1760.
(32) Iluc, V. M.; Hillhouse, G. L. *J. Am. Chem. Soc.* **2010**, *132*, 15148.
(33) Baker, R. T.; Calabrese, J. C.; Harlow, R. L.; Williams, I. D. *Organometallics* **1993**, *12*, 830.
(34) Nakazawa, H.; Yamaguchi, Y.; Mizuta, T.; Ichimura, S.; Miyoshi, K. *Organometallics* **1995**, *14*, 4635.
(35) Menye-Biyogo, R.; Delpech, F.; Castel, A.; Pimienta, V.; Gornitzka, H.; Riviere, P. *Organometallics* **2007**, *26*, 5091.
(36) Takaoka, A.; Mendiratta, A.; Peters, J. C. *Organometallics* **2009**, *28*, 3744.
(37) Wicht, D. K.; Kourkine, I. V.; Lew, B. M.; Nthenge, J. M.; Glueck, D. S. *J. Am. Chem. Soc.* **1997**, *119*, 5039.
(38) Du, D.; Lin, Z.-Q.; Lu, J.-Z.; Li, C.; Duan, W.-L. *Asian J. Org. Chem.* **2013**, *2*, 392.
(39) Ananikov, V. P.; Beletskaya, I. P. *Chem.—Asian J.* **2011**, *6*, 1423.
(40) Ananikov, V. P.; Makarov, A. V.; Beletskaya, I. P. *Chem.—Eur. J.* **2011**, *17*, 12623.
(41) Zhang, Y.; Tang, L.; Pullarkat, S. A.; Liu, F.; Li, Y.; Leung, P.-H. *J. Organomet. Chem.* **2009**, *694*, 3500.
(42) Sugiura, J.; Kakizawa, T.; Hashimoto, H.; Tobita, H.; Ogino, H. *Organometallics* **2005**, *24*, 1099.
(43) Yeo, W.-C.; Tang, L.; Yan, B.; Tee, S.-Y.; Koh, L. L.; Tan, G.-K.; Leung, P.-H. *Organometallics* **2005**, *24*, 5581.
(44) Yeo, W.-C.; Tee, S.-Y.; Tan, H.-B.; Tan, G.-K.; Koh, L. L.; Leung, P.-H. *Inorg. Chem.* **2004**, *43*, 8102.
(45) Han, L.-B.; Zhao, C.-Q.; Tanaka, M. *J. Org. Chem.* **2001**, *66*, 5929.
(46) Zhao, D.; Mao, L.; Yang, D.; Wang, R. *J. Org. Chem.* **2010**, *75*, 6756.
(47) Bravo-Altamirano, K.; Abrunhosa-Thomas, I.; Montchamp, J.-L. *J. Org. Chem.* **2008**, *73*, 2292.
(48) Sadow, A. D.; Togni, A. *J. Am. Chem. Soc.* **2005**, *127*, 17012.
(49) Chen, K.; Pullarkat, S. A.; Ma, M.; Li, Y.; Leung, P.-H. *Dalton Trans.* **2012**, *41*, 5391.
(50) Sabater, S.; Mata, J. A.; Peris, E. *Organometallics* **2013**, *32*, 1112.
(51) Huang, Y.; Pullarkat, S. A.; Li, Y.; Leung, P.-H. *Inorg. Chem.* **2012**, *51*, 2533.
(52) Yang, M.-J.; Liu, Y.-J.; Gong, J.-F.; Song, M.-P. *Organometallics* **2011**, *30*, 3793.
(53) Hoye, P. A. T.; Pringle, P. G.; Smith, M. B.; Worboys, K. *J. Chem. Soc., Dalton Trans.* **1993**, 269.
(54) Blank, N. F.; Moncarz, J. R.; Brunker, T. J.; Scriban, C.; Anderson, B. J.; Amir, O.; Glueck, D. S.; Zakharov, L. N.; Golen, J. A.; Incarvito, C. D.; Rheingold, A. L. *J. Am. Chem. Soc.* **2007**, *129*, 6847.
(55) Rosenberg, L. *ACS Catal.* **2013**, *3*, 2845.
(56) Pringle, P. G.; Smith, M. B. *J. Chem. Soc., Chem. Commun.* **1990**, 1701.
(57) Costa, E.; Pringle, P. G.; Smith, B.; Worboys, M. *J. Chem. Soc., Dalton Trans.* **1997**, 4277.
(58) Costa, E.; Pringle, P. G.; Worboys, K. *Chem. Commun.* **1998**, 49.
(59) Wicht, D. K.; Kourkine, I. V.; Kovacik, I.; Glueck, D. S.; Concolino, T. E.; Yap, G. P. A.; Incarvito, C. D.; Rheingold, A. L. *Organometallics* **1999**, *18*, 5381.
(60) Du, D.; Duan, W.-L. *Chem. Commun.* **2011**, *47*, 11101.
(61) Huang, Y.; Chew, R. J.; Li, Y.; Pullarkat, S. A.; Leung, P.-H. *Org. Lett.* **2011**, *13*, 5862.

(62) Huang, Y.; Pullarkat, S. A.; Li, Y.; Leung, P.-H. *Chem. Commun.* **2010**, *46*, 6950.
(63) Chen, Y.-R.; Duan, W.-L. *Org. Lett.* **2011**, *13*, 5824.
(64) Sues, P. E.; Lough, A. J.; Morris, R. H. *Organometallics* **2012**, *31*, 6589.
(65) Ruiz, J.; Mosquera, M. E. G.; Riera, V.; Vivanco, M.; Bois, C. *Organometallics* **1997**, *16*, 3388.
(66) Riera, V.; Ruiz, J. *J. Organomet. Chem.* **1986**, *310*, C36.
(67) Delavaux, B.; Chaudret, B.; Devillers, J.; Dahan, F.; Commenges, G.; Poilblanc, R. *J. Am. Chem. Soc.* **1986**, *108*, 3703.
(68) Toth, I.; Hanson, B. E.; Davis, M. E. *Organometallics* **1990**, *9*, 675.
(69) Amor, I.; García, M. E.; Ruiz, M. A.; Sáez, D.; Hamidov, H.; Jeffery, J. C. *Organometallics* **2006**, *25*, 4857.
(70) Bandini, A. L.; Banditelli, G.; Minghetti, G. *J. Organomet. Chem.* **2000**, *595*, 224.
(71) Ponomarenko, V. I.; Pilyugina, T. S.; Khripun, V. D.; Grachova, E. V.; Tunik, S. P.; Haukka, M.; Pakkanen, T. A. *J. Organomet. Chem.* **2006**, *691*, 111.
(72) Boettcher, H.-C.; Mayer, P.; Schmidbaur, H. *Z. Naturforsch., B: J. Chem. Sci.* **2012**, *67*, 543.
(73) Gellhaar, J.; Knapp, C. *Acta Crystallogr., Sect. E* **2011**, *67*, o2546.
(74) Atwood, J. L.; Bott, S. G.; Means, C. M.; Coleman, A. W.; Zhang, H.; May, M. T. *Inorg. Chem.* **1990**, *29*, 467.
(75) Rankin, M. A.; Schatte, G.; McDonald, R.; Stradiotto, M. *Organometallics* **2008**, *27*, 6286.
(76) Abdur-Rashid, K.; Fong, T. P.; Greaves, B.; Gusev, D. G.; Hinman, J. G.; Landau, S. E.; Lough, A. J.; Morris, R. H. *J. Am. Chem. Soc.* **2000**, *122*, 9155.
(77) Mazzeo, M.; Lamberti, M.; Massa, A.; Scettri, A.; Pellecchia, C.; Peters, J. C. *Organometallics* **2008**, *27*, 5741.
(78) Bauer, R. C.; Gloaguen, Y.; Lutz, M.; Reek, J. N. H.; de Bruin, B.; van der Vlugt, J. I. *Dalton Trans.* **2011**, *40*, 8822.
(79) Fernández, R.; Melchart, M.; Habtemariam, A.; Parsons, S.; Sadler, P. J. *Chem.—Eur. J.* **2004**, *10*, 5173.
(80) Lehaire, M.-L.; Grundler, P. V.; Steinhauser, S.; Marti, N.; Helm, L.; Hegetschweiler, K.; Schibli, R.; Merbach, A. E. *Inorg. Chem.* **2006**, *45*, 4199.
(81) Gossens, C.; Dorcier, A.; Dyson, P. J.; Rothlisberger, U. *Organometallics* **2007**, *26*, 3969.
(82) Patel, A.; Ludi, A.; Bürgi, H.-B.; Raselli, A.; Bigler, P. *Inorg. Chem.* **1992**, *31*, 3405.
(83) Jayaprakash, K. N.; Conner, D.; Gunnoe, T. B. *Organometallics* **2001**, *20*, 5254.
(84) Maire, P.; Breher, F.; Schönberg, H.; Grützmacher, H. *Organometallics* **2005**, *24*, 3207.
(85) Askevold, B.; Friedrich, A.; Buchner, M. R.; Lewall, B.; Filippou, A. C.; Herdtweck, E.; Schneider, S. *J. Organomet. Chem.* **2013**, *744*, 35.
(86) Trujillo, H. A.; Casado, C. M.; Ruiz, J.; Astruc, D. *J. Am. Chem. Soc.* **1999**, *121*, 5674.
(87) Zhong, Z.; Postnikova, B. J.; Hanes, R. E.; Lynch, V. M.; Anslyn, E. V. *Chem.—Eur. J.* **2005**, *11*, 2385.
(88) Ma, E. S. F.; Mudalige, D. C.; Patrick, B. O.; James, B. R. *Dalton Trans.* **2013**, *42*, 7614.
(89) Jessop, P. G.; Morris, R. H. *Inorg. Chem.* **1993**, *32*, 2236.
(90) Bordwell, F. G. *Acc. Chem. Res.* **1988**, *21*, 456.
(91) Wei, C.; Aigbirhio, F.; Adams, H.; Bailey, N. A.; Hempstead, P. D.; Maitlis, P. M. *J. Chem. Soc., Chem. Commun.* **1991**, 883.
(92) Fan, L.; Wei, C.; Aigbirhio, F. I.; Turner, M. L.; Gusev, O. V.; Morozova, L. N.; Knowles, D. R. T.; Maitlis, P. M. *Organometallics* **1996**, *15*, 98.
(93) Castro, A.; Turner, M. L.; Maitlis, P. M. *J. Organomet. Chem.* **2003**, *674*, 45.
(94) Fairchild, R. M.; Holman, K. T. *Organometallics* **2008**, *27*, 1823.
(95) Fan, L.; Turner, M. L.; Adams, H.; Bailey, N. A.; Maitlis, P. M. *Organometallics* **1995**, *14*, 676.
(96) Koelle, V.; Grub, J. *J. Organomet. Chem.* **1985**, *289*, 133.
(97) Pinkas, J.; Cisarova, I.; Gyepes, R.; Horacek, M.; Kubista, J.; Cejka, J.; Gomez-Ruiz, S.; Hey-Hawkins, E.; Mach, K. *Organometallics* **2008**, *27*, 5532.
(98) Pinkas, J.; Cisarova, I.; Horacek, M.; Kubista, J.; Mach, K. *Organometallics* **2011**, *30*, 1034.
(99) Varga, V.; Sindelar, P.; Cisarova, I.; Horacek, M.; Kubista, J.; Mach, K. *Inorg. Chem. Commun.* **2005**, *8*, 222.
(100) Edelmann, F. T.; Giessmann, S.; Fischer, A. *Chem. Commun.* **2000**, 2153.
(101) Evans, W. J.; Walensky, J. R.; Ziller, J. W. *Chem.—Eur. J.* **2009**, *15*, 12204.
(102) Evans, W. J.; Champagne, T. M.; Ziller, J. W. *J. Am. Chem. Soc.* **2006**, *128*, 14270.
(103) Legzdins, P.; Sayers, S. F. *Organometallics* **1996**, *15*, 3907.
(104) Legzdins, P.; Sayers, S. F. *Chem.—Eur. J.* **1997**, *3*, 1579.
(105) Cloke, F. G. N.; Day, J. P.; Green, J. C.; Morley, C. P.; Swain, A. C. *J. Chem. Soc., Dalton Trans.* **1991**, 789.
(106) Cloke, F. G. N.; Hitchcock, P. B.; Nixon, J. F.; Wilson, D. J. *Organometallics* **2000**, *19*, 219.
(107) Bulls, A. R.; Schaefer, W. P.; Serfas, M.; Bercaw, J. E. *Organometallics* **1987**, *6*, 1219.
(108) Riley, P. N.; Parker, J. R.; Fanwick, P. E.; Rothwell, I. P. *Organometallics* **1999**, *18*, 3579.
(109) Schmiege, B. M.; Fieser, M. E.; Ziller, J. W.; Evans, W. J. *Organometallics* **2012**, *31*, 5591.
(110) Takase, M. K.; Siladke, N. A.; Ziller, J. W.; Evans, W. J. *Organometallics* **2011**, *30*, 458.
(111) Li, C.; Luo, L.; Nolan, S. P.; Marshall, W.; Fagan, P. J. *Organometallics* **1996**, *15*, 3456.
(112) Kolle, U.; Kang, B.-S.; Thewalt, U. *J. Organomet. Chem.* **1990**, *386*, 267.
(113) Burn, M. J.; Fickes, M. G.; Hollander, F. J.; Bergman, R. G. *Organometallics* **1995**, *14*, 137.
(114) Geldbach, T. J.; Drago, D.; Pregosin, P. S. *Chem. Commun.* **2000**, 1629.
(115) Geldbach, T. J.; Pregosin, P. S.; Bassetti, M. *Organometallics* **2001**, *20*, 2990.
(116) Tan, X.; Li, B.; Xu, S.; Song, H.; Wang, B. *Organometallics* **2011**, *30*, 2308.
(117) Bennett, D. W.; Siddiquee, T. A.; Haworth, D. T.; Kabir, S. E.; Hyder, M. I.; Ahmed, S. J. *J. Chem. Crystallogr.* **2004**, *34*, 361.
(118) Bruce, M. I.; Humphrey, P. A.; Okucu, S.; Schmutzler, R.; Skelton, B. W.; White, A. H. *Inorg. Chim. Acta* **2004**, *357*, 1805.
(119) Bott, S. G.; Shen, H.; Richmond, M. G. *J. Organomet. Chem.* **2004**, *689*, 3426.
(120) Crochet, P.; Demerseman, B.; Rocaboy, C.; Schleyer, D. *Organometallics* **1996**, *15*, 3048.
(121) Boren, B. C.; Narayan, S.; Rasmussen, L. K.; Zhang, L.; Zhao, H.; Lin, Z.; Jia, G.; Fokin, V. V. *J. Am. Chem. Soc.* **2008**, *130*, 8923.
(122) Frisch, M. J.; et al. *Gaussian 09*, revision B.01; Gaussian, Inc.: Wallingford, CT, 2010.
(123) Kulkarni, A. D.; Truhlar, D. G. *J. Chem. Theory Comput.* **2011**, *7*, 2325.
(124) Zhao, Y.; Truhlar, D. G. *Theor. Chem. Acc.* **2008**, *120*, 215.
(125) Zhao, Y.; Truhlar, D. G. *J. Chem. Phys.* **2006**, *125*, No. 194101.
(126) Leininger, T.; Nicklass, A.; Stoll, H.; Dolg, M.; Schwerdtfeger, P. *J. Chem. Phys.* **1996**, *105*, 1052.
(127) Andrae, D.; Häußermann, U.; Dolg, M.; Stoll, H.; Preuß, H. *Theor. Chim. Acta* **1990**, *77*, 123.
(128) Clark, T.; Chandrasekhar, J.; Spitznagel, G. W.; Schleyer, P. v. R. *J. Comput. Chem.* **1983**, *4*, 294.
(129) Lynch, B. J.; Zhao, Y.; Truhlar, D. G. *J. Phys. Chem. A* **2003**, *107*, 1384.
(130) Frisch, M. J.; Pople, J. A.; Binkley, J. S. *J. Chem. Phys.* **1984**, *80*, 3265.
(131) Tomasi, J.; Mennucci, B.; Cammi, R. *Chem. Rev.* **2005**, *105*, 2999.
(132) Tomasi, J.; Mennucci, B.; Cancès, E. *J. Mol. Struct. (THEOCHEM)* **1999**, *464*, 211.

(133) Marenich, A. V.; Cramer, C. J.; Truhlar, D. G. *J. Phys. Chem. B* **2009**, *113*, 6378.
(134) Fukui, K. *Acc. Chem. Res.* **1981**, *14*, 363.
(135) Nagashima, K. *J. Magn. Reson.* **2008**, *190*, 183.